APPLICATIONS OF ARTIFICIAL INTELLIGENCE AND DEEP LEARNING FOR SUSTAINABLE WATER MANAGEMENT IN PRINCE EDWARD ISLAND

A Thesis

Submitted to the Graduate Faculty

in Partial Fulfilment of the Requirements

for the Degree of Master of Science

Sustainable Design Engineering

Faculty of Sustainable Design Engineering

University of Prince Edward Island

Hassan Afzaal

Charlottetown, Prince Edward Island

March 2020

THESIS/DISSERTATION NON-EXCLUSIVE LICENSE

Family Name: Afzaal	Given Name, Middle Name (if applicable): Hassan
Full Name of University: University of Prince Edward Island	
Faculty, Department, School: Faculty of Sustainable Design Engineering	
Degree for which thesis/dissertation was presented: M. Sc, Sustaible Design Engineering	Date Degree Awarded:
Thesis/dissertation Title: APPLICATIONS OF ARTIFICIAL INTELLIGENCE AND DEEP LEARNING FOR SUSTAINABLE WATER MANAGEMENT IN PRINCE EDWARD ISLAND	
Date of Birth. It is **optional** to supply your date of birth. If you choose to do so please note that the information will be included in the bibliographic record for your thesis/dissertation. 18 December, 1992	

In consideration of my University making my thesis/dissertation available to interested persons, I,

---

hereby grant a non-exclusive, for the full term of copyright protection, license to my University, The university of Prince Edward Island:

(a) to archive, preserve, produce, reproduce, publish, communicate, convert into any format, and to make available in print or online by telecommunication to the public for non-commercial purposes;
(b) to sub-license to Library and Archives Canada any of the acts mentioned in paragraph (a).

I undertake to submit my thesis/dissertation, through my University, to Library and Archives Canada. Any abstract submitted with the thesis/dissertation will be considered to form part of the thesis/dissertation.

I represent that my thesis/dissertation is my original work, does not infringe any rights of others, including privacy rights, and that I have the right to make the grant conferred by this non-exclusive license.

If third party copyrighted material was included in my thesis/dissertation for which, under the terms of the *Copyright Act*, written permission from the copyright owners is required I have obtained such permission from the copyright owners to do the acts mentioned in paragraph (a) above for the full term of copyright protection

I retain copyright ownership and moral rights in my thesis/dissertation, and may deal with the copyright in my thesis/dissertation, in any way consistent with rights granted by me to my University in this non-exclusive license.

I further promise to inform any person to whom I may hereafter assign or license my copyright in my thesis/dissertation of the rights granted by me to my University in this non-exclusive license.

Signature [redacted]	**Date** 26 June, 2020

University of Prince Edward Island

Faculty of Sustainable Design Engineering

Charlottetown

CERTIFICATION OF THESIS WORK

We, the undersigned, certify that , candidate for the degree of Master of Science in Sustainable Design Engineering has presented a thesis with the following title: "Applications of Artificial Intelligence and Deep Learning for Sustainable Water Management in Prince Edward Island", that the thesis is acceptable in form and content, and that a satisfactory knowledge of the field covered by the thesis was demonstrated by the candidate through an oral examination held on May 27, 2020

Examiners: Dr. Aitazaz Farooque [redacted]

Dr. Bishnu Acharya [redacted]

Dr. Travis Esau [redacted]

Dr. Xander Wang [redacted]

Dr. Amy Hsiao - Chair [redacted]

Date May 27, 2020

ABSTRACT

Precision agriculture evaluates and quantifies the input needs of crops for their optimum yield and sustainable production. Growth of potato plants is highly sensitive to drought conditions, which drastically reduce tuber yield if precision supplemental irrigation (SI) is not provided. The hypothesis of this study, that the rainfall in Prince Edward Island is not enough for sustainable potato production in the island, was tested under three specific objectives including i) to model evapotranspiration with artificial intelligence for precision water resource management, ii) to determine the effects of different irrigation systems (sprinkler, drip, fertigation and control; rainfed) on potato tuber yield, quality, payout returns, and iii) to model the groundwater levels of Prince Edward Island using deep learning methods to ensure sustainability of water balance in Prince Edward Island.

This study used deep learning, artificial neural networks (ANNs) and the standard hydrology models to estimate components of water cycle for their use and impact on potato production in Prince Edward Island. Reference evapotranspiration was estimated with recurrent neural networks (RNNs) namely long short term memory (LSTM) and Bidirectional LSTM. Four representative meteorological sites (North Cape, Summerside, Harrington and Saint Peters) were selected across the island. Crop specific evapotranspiration (ETc) was calculated from reference evapotranspiration (ET_O) using Penman Monteith equation, FAO-56 method, ANNs, and RNNs, and LSTMs. Based on subset regression analysis, the highest contributing climatic variables namely maximum air temperature and relative humidity were selected as input variables for RNNs' training (2011-2015) and testing (2016-2017) runs. The results suggested that the LSTM and

Bidirectional LSTM are suitable methods to accurately ($R^2 > 0.90$) estimate ET_O for all sites except for Harrington. No major differences were observed in the accuracy of LSTM and Bidirectional LSTM. The potential gap between ET_O and rainfall were highlighted for assessing agriculture sustainability in Prince Edward Island. Analyses of the data highlighted that the cumulative ET_O surpassed the cumulative rainfall potentially affecting yield of major crops in the island. Therefore, agriculture sustainability requires viable options such as SI to replenish the crop water requirements as and when needed. Results suggested that July, August, and September are relatively drier months of the study years and SI may be required to meet the crop water requirements.

In order to evaluate impact of SI, pressurized irrigation systems including sprinkler, fertigation and drip irrigation were installed at small-scale to offset deficit in soil moisture as compared to conventional practice of rainfed conditions, i.e., no irrigation practice (control). Significant differences in potato yield were observed between control and irrigation methods used in this study. A two-way ANOVA was run to examine the effect of irrigation methods and year on potato tuber yield, water productivity, tuber quality, and payout. In term of payout returns the sprinkler treatment performed significantly better than control, drip, and fertigation in 2018. However, in terms of water productivity, the fertigation treatment performed significantly better than the control and sprinkler treatments during both growing seasons. The lower water productivity of sprinkler irrigation was due to higher water consumption in comparison with drip and fertigation systems.

Needs of SI for potato production in Prince Edward Island can be met from groundwater pumping. This necessitates the budgeting of water cycle components for efficient

management of water resources. In areas where groundwater pumping is common for SI or for domestic use, the inventory control of groundwater resources could become more convenient with the use of deep learning, ANNs, and RNNs namely a multilayer perceptron (MLP) and LSTM. The analysis of two watersheds namely Baltic and Long creep showed that the deep learning methods used in this study are accurate to simulate groundwater levels. Input variables for this watershed-scale modelling investigation included stream level, streamflow, precipitation, relative humidity, mean temperature, heat degree days, dew point temperature, and ETo. Using a hit and trial approach and various hyperparameters, all ANNs were trained from scratch (2011–2015) and validated (2016–2017). The stream level was the major contributor to GWL fluctuation for the Baltic River and Long Creek watersheds (R^2 = 0.508 and 0.491 respectively). The MLP performed better in validation for Baltic River and Long Creek watersheds (RMSE = 0.471 and 1.15, respectively). The deep learning techniques introduced in this study to estimate GWL fluctuations are convenient and accurate as compared to collection of periodic dips based on the groundwater monitoring wells for groundwater inventory control and management.

ACKNOWLEDGEMENTS

First, I want to dedicate a special gratitude to my supervisor, Dr. Aitazaz Farooque, under whose kind and insightful supervision, I was able to accomplish this research work. He always remains an inspiration and role model for me. His professional commitment, kind behavior and way of teaching motivated me to work hard. His clear approach guided me towards right direction to achieve more in less time. I would also like to pay my thanks to my supervisory committee mentor; Dr. Bishnu Acharya and Dr. Travis Esau for their continuous guidance and support. I would also like to dedicate a special gratitude to Dr. Farhat Abbas for detailed and critical review of my thesis. His thought provoking corrections, valuable suggestions and throughout guidance made significant improvements in my thesis.

I will never forget the contributions of Andrew MacEwen, Nazar Hussain, Charles Terrio, William Hardy and research team at UPEI for their help in installing irrigation system, data collection and assistance throughout the experiment.

I am very thankful to my mother who facilitated me morally at every step as without her affection, psychological support and prayers I may not continue the research work with full devotion and attention. I cannot ignore the encouragements from my sisters at all levels.

I would not be able to end my acknowledgements without recognizing that ultimately it has been by the grace of Almighty God, and I must gratefully submit my thanks and praises to Him for any good that comes into my life.

TABLE OF CONTENTS

LIST OF FIGURES

LIST OF TABLES

LIST OF ABBREVATIONS AND SYMBOLS USED

Aerodynamic resistance (Y_a)

Analysis of variance (ANOVA)

Artificial intelligence (AI)

Area (A)

Artificial neural networks (ANNs)

Actual value at the *i*th time (y_i)

Actual yield (Ya)

Applied irrigation (I)

Crop evapotranspiration (ETc)

Coefficient of determination (R^2)

Crop development factor (kc)

Convolutional neural network (CNN)

Combine state (C_t)

Change in storage (ΔS)

Deep learning (DL)

Difference of pairs of means ($M_i - M_j$)

Evapotranspiration (ET)

Estimated value at the *i*th time ($\hat{y}_i$)

Estimation of model (X_{ijk})

Errors (ε_{ijk})

Food and Agriculture Organization (FAO)

Forget gate of LSTM (f_t)

Groundwater levels (GWL)

Honest significant difference (HSD)

Input gate of LSTM (X_t)

Interaction effect (γ_{ij})

Long short term memory (LSTM)

Levenberg Marquardt (LM)

Mean daily mean temperature (Tmean)

Multilayer perceptron (MLP)

Mean air density at constant air pressure (ρ_a)

Mean of i,j group (μ_{ij})

Main effects (α_i, β_j)

Mean square with group (MS_w)

Number in treatments (n)

Net radiation (R_n)

Overall mean (μ)

Output gate of LSTM (o_t)

Precipitation (P)

Psychrometric constant (Y)

Runoff (Q)

Reference evapotranspiration (ETo)

Recurrent neural networks (RNNs)

Root means square error (RMSE)

Supplemental irrigation (SI)

Standardized Penman-Monteith (FAO-56)

Soil heat flux (G)

Specific heat of the air (C_p)

Surface resistance (Y_s)

Vapor saturation pressure (Δ)

Vapor pressure deficit (es – ea)

Velocity (V)

Wind speed (U)

CHAPTER 1
INTRODUCTION

Potato industry significantly promotes the economy of Prince Edward Island as it contributes about 10.8% to the GDP (gross domestic product) of this province with more than one billion direct and indirect economic benefits engaging 12.1% of total work force of the island [1]. Currently, Prince Edward Island produces approximately 20-25% of total potatoes grown by Canada each year [2]. Potato is very sensitive crop in terms of yield and quality under limited water conditions [3]; therefore, the soil water should not be depleted by more than 30-50% for optimum potato yield [4-5].

Precision agriculture does not only evaluate and quantify the input needs of crops for their optimum yield and sustainable production but also assesses risks if the crop inputs are not scientifically managed. The findings of study by Shock et al. [6] suggested the higher risk of reduced potato yields in case of scarce soil water. Since, the majority of potato production in Prince Edward Island is rainfed, the irregular rainfall pattern may affect potato yield. Furthermore, climate changes add severity to this problem as more hot days, lesser cold days and changing precipitation patterns are predicted for next decades [7]. These challenges demand the precise quantification of plant water requirements, calculated from reference evapotranspiration (ETo), through the use of robust and accurate artificial intelligent techniques.

Based on the computed ETo and rainfall gaps found during preliminary modeling of physical hydrology components of Prince Edward Island, this study compared the effects of supplemental irrigation (SI) on potato tuber yield, quality, payout returns and water productivity. Several irrigation methods have been tested previously to replenish the crop

water requirements on need basis; however, there are no clear guidelines for this region for selection of appropriate irrigation method for sustainable production in the island.

Over the past few years, there has been increased demand in the agriculture sector for SI, which poses several challenges for water and resource managers. Because of the relatively small and non-contiguous watersheds in Prince Edward Island, pumping of groundwater has also raised concerns for groundwater sustainability due to the island's uneven topography [8]. An inventory of groundwater is necessary for efficient water resource management, especially in relation to growing groundwater demands for agricultural use. It is neither feasible nor economical to install and manage monitoring groundwater wells in a place like Prince Edward Island, which consists of 260 watersheds for efficient water management. The inventory control of the groundwater resource can ensure the sustainability of water resources in the areas where groundwater pumping is common for supplemental irrigation or for domestic use.

The hypothesis built in this study was that the rainfall in Prince Edward Island is not enough for sustainable potato production in the island. Several deep learning models have been tested to highlight the gaps between rainfall and ETo. Irrigation methods namely drip, sprinkler and fertigation were tested in consideration with potato tuber yield, quality, and payout returns. Furthermore, to evaluate the effect of supplemental irrigation on groundwater levels; several deep learning methods have been tested for inventory of the water cycle components.

1.1 Study Objectives

The objectives of this study were:

1. To model evapotranspiration with artificial intelligence for precision water resource management.
2. To determine the effects of different irrigation systems (sprinkler, drip, fertigation, and control; rainfed) on potato tuber yield, quality, payout returns.
3. To model the groundwater levels of Prince Edward Island using deep learning methods to ensure sustainability of water balance in Prince Edward Island.

1.2 Thesis Structure

This document follows the publication style thesis in which first chapter explains the brief introduction of each objective. Chapters 2-4 report the results of modeling and field work to achieve the three study objectives, respectively. Each chapter has its own specific abstract, introduction, material and methods, results, and discussion. Chapter 5 summarizes the results presented in Chapters 2-4.

In chapter 2, several methods were tested to quantify the crop water requirements and rainfall gaps for agricultural sustainability in Prince Edward Island. The tested methods in this study were more accurate and required less input variables for estimation of crop water requirements. This study is published in peer reviewed *Applied Sciences* Journal, (https://www.mdpi.com/2076-3417/10/5/1621).

After identifying gaps between crop water requirements and rainfall (Chapter 3); three different irrigation methods namely drip, sprinkler and fertigation were tested to evaluate the potato crop suitability in context with potato tuber yield, quality and payout

returns. This study is also published in peer reviewed *Sustainability* Journal (https://www.mdpi.com/2071-1050/12/6/2419).

To evaluate the irrigation impacts on groundwater levels, three deep learning methods namely multilayer perceptron, recurrent neural networks and convolutional neural networks were tested with varying input combinations to estimate the fluctuation in ground water. This study is published in peer reviewed *Water* Journal (https://www.mdpi.com/2073-4441/12/1/5).

1.3 Author Contributions

This is a publication-based thesis that includes the ideation, review and help of student's committee members in writing process of the publications made part of this thesis. All the writing, experiments, data collection, and data analysis techniques used in this study have been conducted by the master's degree candidate himself. The committee members helped the candidate in ideation of objectives and improved the quality of these presentations for multiple times. To recognize the contributions of committee members; all committee members were included in the authorship lists of the peer reviewed articles based on their contributions.

CHAPTER 2

Computation of Evapotranspiration with Artificial Intelligence for Precision Water Resource Management

Abstract

Accurate estimation of evapotranspiration provides useful information for water resource management, irrigation planning and crop sustainability. This study estimates the reference evapotranspiration with recurrent neural networks namely long short term memory (LSTM) and Bidirectional LSTM. Four representative meteorological sites (North Cape, Summerside, Harrington and Saint Peters) were selected across Prince Edward Island (PEI), Canada to form a PEI database from mean values of the four sites' climatic variables to capture climatic variability from all parts of the province. The highest contributing climatic variables namely maximum air temperature and relative humidity were selected based on subset regression analysis as input variables for RNNs' training (2011-2015) and testing (2016-2017) runs. The results suggested that the LSTM and Bidirectional LSTM are suitable methods to accurately ($R2 > 0.90$) estimate reference evapotranspiration for all site except Harrington. Testing period (2016-2017) root mean square errors were recorded in range of 0.38-0.58 mm/day for all sites. No major differences were observed in accuracy of LSTM and Bidirectional LSTM. Another objective of this study was to highlight the potential gap between reference evapotranspiration and rainfall for assessing agriculture sustainability in Prince Edward Island. Analyses of the data set 2011-2017 highlighted that the cumulative reference evapotranspiration surpassed the cumulative rainfall potentially affecting yield of major

crops in the island. Therefore, agriculture sustainability requires viable options such as supplemental irrigation to replenish the crop water requirements as and when needed.

2.1 Introduction

Evapotranspiration (ET) is key element in water balance as well as surface energy equation. Accurate estimation of ET provides useful information for water resource management, irrigation planning and crop sustainability. Lysimeters are commonly used in estimation of ET directly; however, the use of lysimeters in ET estimation is very limited because of high maintenance and operational costs [9]. Several mathematical models indirectly estimate ET and are considered to be the intelligent alternative of direct methods due to time saving and ease of application [10]. Standardized Penman-Monteith (FAO-56) is the most acceptable mathematical model for estimation of ET_O [11].

Under both humid and arid climatic conditions, FAO-56 method has been unanimously reported to be the most efficient method for estimation of ET_O by incorporating thermodynamic as well as aerodynamic effects [12]. However, input data needed by FAO-56 method including temperature, relative humidity, solar radiation, wind speed and more information about the area makes its applicability challenging for several locations across the globe. Solutions to this problem have been sought by introducing various empirical methods through simplifying the FAO-56 method, such as, Hargreaves equation that requires temperature data only to estimate ET_O. The choice of methods solely depends upon the accuracy of methods and availability of reliable data. An ideal method however should be based on minimal input data variables with no compromise on precision and accuracy [13].

Artificial neural networks (ANNs) have drawn the attention of researchers to model the complex non-linear hydrological relationships. Several ANNs have been successfully used to solve hydrology related problems such as river flows extrapolation [14], rainfall run-off modelling [15] sediment forecasting [16], and notably ET_O [17]. Afterwards, several improvements in ANN's architecture, learning algorithms have been proposed by different researchers. For example, Sudheer et al. [18] modelled the ET_O for rice crop. They used radial basis neural networks with varied combinations of climatic input variables. Aytek et al. [19] proposed the explicit neural network to model the ET_O by using daily climatic variables in California, USA by comparing six different conventional methods. Rahimikhoob [20] trained the ET models by using only air temperature of Caspian Sea in North Iran and compared their results with FAO-56 model output. They concluded that the air temperatures were able to explain the variability in ET without compromising the accuracy. In recent years, several other machine learning models were tested to estimate ET_O such as extreme learning machines [10,21,22], support vector machines [18] and Fuzzy genetic approach [23]. Several climatic variables such as temperature, relative humidity and ET exhibit seasonality and may be treated as a time series problem. Although, ANNs handle the non-linear behavior of time series better than regular regression; however, most of the ANNs do not explain seasonality and time dependence. Simple ANN architecture such as multilayer perceptron does not contain any memory blocks to store the previous information for better prediction. To address this issue, recurrent neural networks (RNNs) were introduced to capture the dynamics of sequences via cycles in the network of nodes [24].

In RNNs, the temporal relations of inputs are addressed by feedback connections for maintaining internal memory states. Recurrent neural networks have proved to be effective in learning time dependent signals for short term structure [25]. They are capable of storing previous records in their memory. However, in large time series sequences the vanishing gradient hampers the learning of these models. This problem occurs when gradient updates become very small and add no major contribution towards model learning. Long short term memory (LSTM) neural networks were introduced to overcome the vanishing gradient problems of RNNs with capability of storing important information containing long sequences [26]. To further improve the performance of RNNs, more advance LSTM were developed by Schuster and Paliwal [27] named bidirectional LSTM. The LSTMs relate different past records in time series problems; however, in bidirectional LSTMs the enhanced learning mechanism enable them to relate the past as well as future records for better estimation of a variable. The LSTMs are used in a number of applications including speech recognition, time series predictions and grammar learning. However, the application of LSTMs in the field of hydrology has not been widely reported in literature but can be used in estimation of hydrologic variables since several climatic variables used in hydrology exhibit time series behavior. Several studies have highlighted the potential of LSTMs in rainfall runoff modelling [28-29] in which the performance of LSTMs was better than physically based runoff models. Zhang et al. [30] used LSTMs for groundwater estimation and reported that they performed better than multilayer perceptron model. They used the dropout effect in hidden layers of LSTMs to increase the model learning for better estimation of groundwater. However, based on literature review, the use of advanced RNNs in ET_O modelling is very limited and/or unpublished. Therefore, this study explores the

performance of conventional LSTMs and bidirectional LSTMs in modeling ET_O across Prince Edward Island, Canada with the specific objectives to i) model ET_O with high accuracy as well as with reduced number of variables and ii) identify the need of supplemental irrigation by comparing the rainfall and estimated ET_O for sustainable production of potatoes in Prince Edward Island.

Need for this study is based on the fact that out of 57 meteorological sites installed in Prince Edward Island, less than 10 sites provide enough data for ET_O estimation using FAO-56 method. This leaves researchers and the Government sectors responsible to promote sustainable agriculture in the island to look for other approaches of estimating ET_O to guide farmers about making intelligent decisions about irrigating their crops. The neural networks and analysis used in this study to estimate the ET_O have not been previously used and/or published for this region makings this study novel innovative for scientific community and Government sectors involved in agricultural activities.

2.2 Experiments and Methods

2.2.1 Site Selection

The Atlantic Canadian province of Prince Edward Island is situated in the Gulf of Saint Lawrence and separated from the other Atlantic provinces namely Nova Scotia and New Brunswick at Northumberland Strait. Four meteorological sites were selected across the island to represent climatic conditions of the whole island (Figure 2-1). For example, North Cape (47.058056 ^{0}N 63.998611 ^{0}W) was selected to represent the west part of the island. Summerside (46.441111 ^{0}N 63.838056 ^{0}W) and Harrington (46.343617 ^{0}N 63.169736 ^{0}W) meteorological sites were selected to represent the central parts of the island. Saint Peter

(46.450278 ^{0}N 62.575833 ^{0}W) meteorological station represented eastern parts of the island.

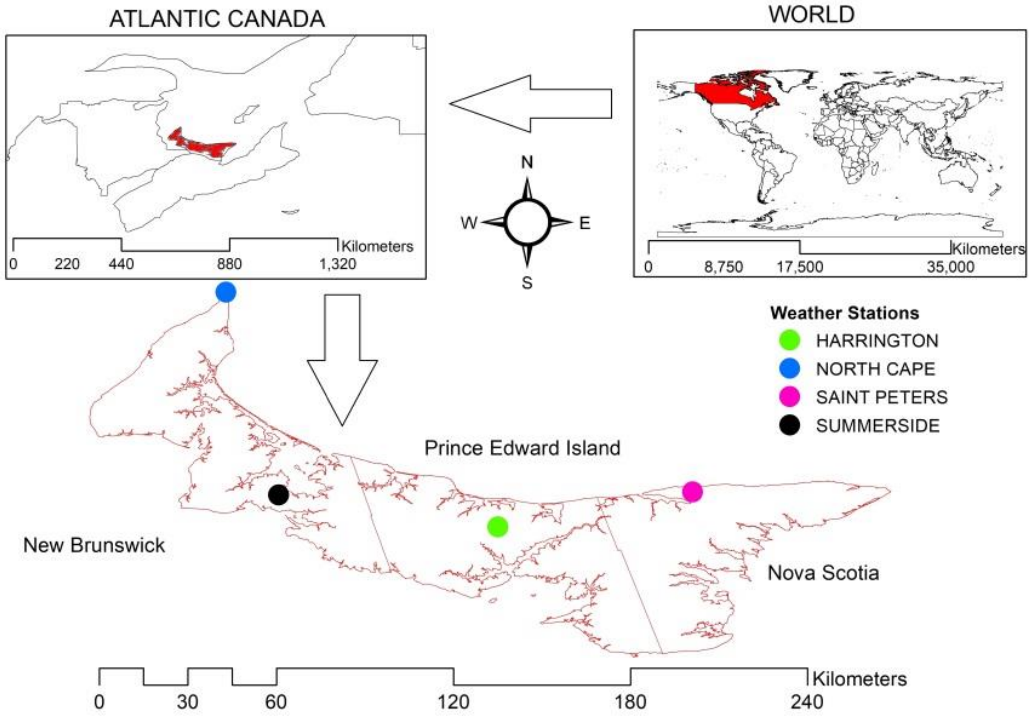

Figure 2-1 Locations of the four selected meteorological stations across Prince Edward Island, Canada

2.2.2 Data Collection and Variable Selection

Daily climatic data of four selected meteorological sites for period 2011-2017 was retrieved from Environment Canada historical database. Initially, nine different variables namely heat degree days, hourly mean air temperature, minimum air temperature, maximum air temperature, relative humidity, dew point temperature, wind speed, atmospheric pressure and daily mean air temperature were selected. To capture the variation of climatic variables from different part of the island, a new dataset (Prince Edward Island database) was formed by averaging the variables of all four sites.

Regression subset analysis was conducted with varied input combinations to select the appropriate inputs for artificial intelligence models. ET_O was selected as response variable and regressed with nine selected climatic variables. Minitab (Version 18) was used to conduct subset regression analysis. Best subset regression fits all the possible combination based on independent variables. However, for simplicity only the best performing variable based on highest coefficient of determination among varied input combinations were selected (Table 2-1).

2.2.3 Penman-Monteith FAO-56 Model

Actual ET_O data were not available for the selected study sites; therefore, FAO-56 method was used to estimate the ET_O for these sites. The estimated ETo from FAO-56 method was used as targets for LSTMs and bidirectional LSTM neural networks. The FAO-56 model is accepted and has been widely used [11,31,32] in these situations. The Penman-Monteith equation for ET_O estimation is expressed as:

$$\mathrm{ETo}\left(\frac{\mathrm{mm}}{\mathrm{day}}\right) = \frac{\Delta(\mathrm{R_n} - \mathrm{G}) + \rho_a c_p \left(\frac{\mathrm{es} - \mathrm{ea}}{\mathrm{ra}}\right)}{\Delta + \gamma\left(1 + \frac{\mathrm{r_s}}{\mathrm{r_a}}\right)} \qquad (2-1)$$

The Penman-Monteith equation was derived in most acceptable form by Allen et al. [11] also known as FAO-56 model expressed as:

$$\mathrm{ETo}\left(\frac{\mathrm{mm}}{\mathrm{day}}\right) = \frac{0.408\Delta(\mathrm{R_n} - \mathrm{G}) + \gamma\left(\frac{900}{\mathrm{Tmean} + 271}\right)\mathrm{U}(\mathrm{es} - \mathrm{ea})}{\Delta + \gamma(1 + 0.34\mathrm{U})} \qquad (2-2)$$

where Δ is the slope of the vapor saturation pressure, R_n is the net radiation, G is the soil heat flux, ρ_a is the mean air density at constant air pressure, C_p is the specific heat of the air, es − ea is the vapor pressure deficit, Y is the psychrometric constant, U is wind speed

at 2 meter (m/s), Tmean is daily mean temperature, Y_s is the surface resistance, and Y_a is the aerodynamic resistance m.

2.2.4 Long Short Term Memory Neural Networks

The RNNs are sequence-based model, equipped with memory blocks to store and relate the previous information in a sequence. However, vanishing gradient hinders the learning in earlier layers of RNNs and this phenomenon is sometimes referred as short term memory. Input (X_t), output (o_t) and forget (f_t) gates were added in memory blocks of LSTMs to address short term memory problems. The forget gate has ability to discard irrelevant information based on relevance, i.e., the input variables after normalization closer to 0 are forgotten and closer to 1 are kept for further use. Forget gate in LSTMs reduces the chances of overfitting by not carrying outall information from the previous steps. Selective information control in LSTM is the key reason to overcome the vanishing gradient problems and making them suitable for non stationary data modelling.

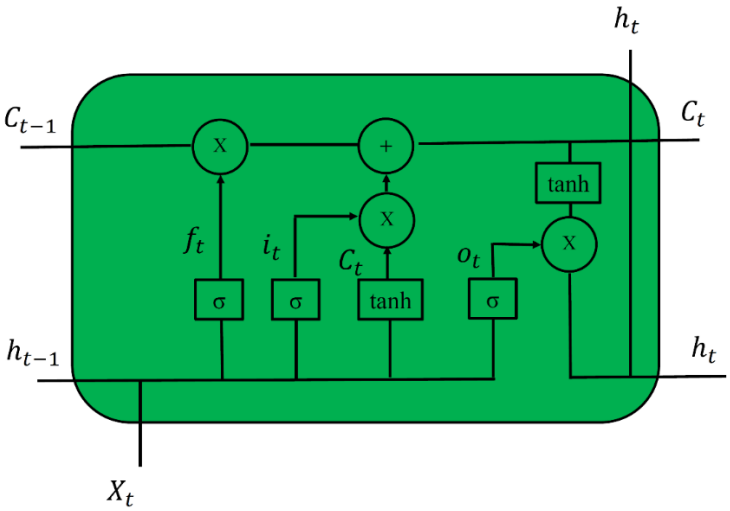

Figure 2-2 The memory block of long short term memory (LSTM) neural networks.

After passing through f_t, tanh and sigmoid functions are used to scale the values for further processing. Combine state (C_t) is computed as a result of dot product between tanh and sigmoid outputs. The more detailed overview of LSTM information flow memory block is described in Figure 2-2.

2.2.5 Bidirectional Long Short Term Memory Neural Networks

Bidirectional LSTMs have two way information flow in contrast with traditional LSTM (Figure 2-3). Bidirectional LSTMs can relate information from previous as well as future time steps making them more powerful than traditional LSTMs. The outputs from both directions then aggregate for labels prediction.

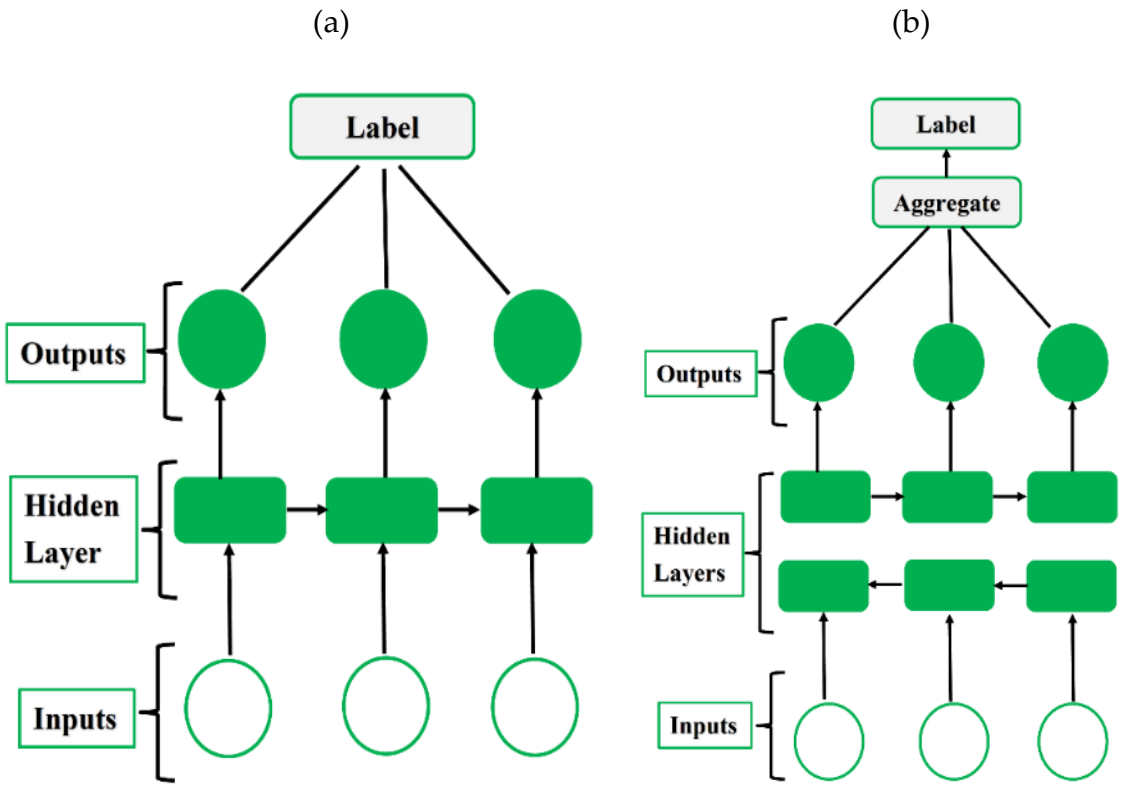

Figure 2-3 The basic structure of RNN (a) LSTM, (b) Bidirectional LSTM

2.2.6 Hyperparameter Tuning and Reproducibility

Daily meteorological variables were split in training (2011-2015) and testing (2016-2017) sets. The test sets were used to estimate the ET_0 after successful (convergence) training of the models. Extensive tests were performed to determine the hyperparameters of LSTMs. Several hyperparameters including neurons, learning rates, optimizers, batch sizes and dropout effects were tested for higher accuracy. The highest performing learning rates, neuron and batch sizes were used in models training and testing. Due to large data points used in this study, several data normalization techniques were tested to reduce the noise effects in data. The max-min normalization performed better with our data in comparison with other data normalization functions. After training of models, the data were back transformed to original scale.

TensorFlow framework was selected because of its wide applications in industrial deployment. Several libraries including Keras with TensorFlow backend, Numpy, Matplotlib, Pandas and Scikitlearn was used with Python programming language. All models were trained using Dell Latitude 5580 workstation, with Intel Core I7 7600U CPU, 8GB ram, Nvidia GeForce 930MX and Ubuntu 16.04 X64 operating system. Furthermore, for reproduceable results, seeds for random number generators were preset. For examples, Python-hash seeds were set to 0, for Numpy the random seeds were set to 111, Python random seeds were set to 10 and TensorFlow random seeds were set to 89. All the results displayed in this study were retrieved using above mentioned random seed configuration.

2.2.7 Rainfall Evapotranspiration Comparison

Evapotranspiration is considered to be the prominent parameter in water balance equation, which is expressed as:

$$P=Q+ET+\Delta S \quad (2\text{-}3)$$

Where P is precipitation, Q is runoff, ET is evapotranspiration and ΔS represented as storage in soil. Over the longer periods, changes in water storage for particular region may be neglected [33] and precipitation is balanced by runoff and ET only. Furthermore, in agricultural the land runoff has minor effects on water balance equation because of higher infiltration rates in soil. This study aims to compare the rainfall and ET_O only on province scale without considering the effect of runoff and change in storage. Planting season (June-November) was considered only to compare with rainfall with ET_O, as the agriculture is not possible in winter season [34] in Prince Edward Island because of snow and colder weather.

2.2.8 Model Evaluation

Loss of the model was evaluated by mean absolute error (MAE), which is the average of all absolute errors between predictions and labels. MAE is expressed as:

$$\text{MAE} = \frac{1}{N}\sum_{i=1}^{N}|y_i - \hat{y}i| \quad (2-4)$$

The root means square error (RMSE) and coefficient of determination (R^2) were also used to evaluate the model effectiveness. RMSE has been used in various studies to evaluate the neural networks predictive power. Coefficient of determination (R^2) is well

known model evaluation measure. Values of R^2 closer to 1 represent the models with higher predictive power. RMSE and R^2 can be defined as:

$$\text{RMSE} = \sqrt{\frac{\sum_{i=1}^{N}(yi - \hat{y}i)^2}{N}} \qquad (2-5)$$

$$R^2 = \sqrt{\frac{\sum_{i=1}^{N}(yi - \bar{y})^2 - \sum_{i=1}^{N}(yi - \hat{y}i)^2}{\sum_{1=1}^{N}(yi - \bar{y})^2}} \qquad (2-6)$$

where y_i is the actual value at the *i*th time, $\hat{y}_i$ is the estimated value at the *i*th time, and *i* ranges from 1 to *N*. $|y_i - \hat{y}i|$ are the absolute error between actual and predicted values at *i*th time.

2.3 Results and Discussion

2.3.1 Selection of Climatic Variables

The results of subset regression analysis suggested that the maximum air temperature was the highest contributor among selected variables in estimation of ET_O. For all sites, R^2 was in the range of 70.7-74.4% between ET_O and maximum air temperature. Higher R^2 indicated the strong predictive of maximum air temperature in estimation of ET_O. A study by Feng et al. [35] explained the significance of temperature data in reference to ET modelling. They used only temperature data to estimate the ET_0. These results are in agreement with the findings of Feng et al. [35] and confirmed the relevance of temperature data for modeling ET_O. Relative humidity was the second largest contributor in estimation of ET_O as it increased the R^2 by 0.11, 0.13, 0.14, 0.10, and 0.12 for Saint Peter, Harrington, North Cape, Summerside and Prince Edward Island data sets, respectively (Table 2-1). By increasing the number of variables from 2 to 5, there were minor increases of 0.22, 0.013, 0.024, 0.016, and 0.021 in R^2 for Saint Peter, Harrington, North Cape, Summerside, and

Prince Edward Island data sets, respectively. Based on subset regression analysis results, only two variables namely maximum air temperature and relative humidity were selected in training of recurrent neural networks.

Table 2-1 Subset Regression Analysis regressed versus FAO-56 ETo

Site	Variable (Number)	R^2	[1]HDD	[2]Hourly Mean Air Temp (°C)	[3]Min. Air Temp (°C)	[4]Max. Air Temp (°C)	Relative Humidity (%)	[5]Dew Point Temp (°C)	[6]Daily Mean Air Temp (°C)
Saint Peters	1	71.9				X			
	2	83.0				X	X		
	3	83.9				X		X	X
	4	84.6	X			X		X	X
	5	85.2	X	X		X		X	X
Harrington	1	70.7				X			
	2	83.9				X	X		
	3	84.4				X		X	X
	4	84.8	X			X		X	X
	5	85.2	X	X		X		X	X
North Cape	1	72.5				X			
	2	87.0				X	X		
	3	88.0				X		X	X
	4	88.8	X	X		X	X		
	5	89.4	X	X		X		X	X
Summerside	1	73.6				X			
	2	83.6				X	X		
	3	84.2				X		X	X
	4	84.7	X			X		X	X
	5	85.2	X		X	X		X	X
Prince Edward Island	1	74.4				X			
	2	86.2				X	X		
	3	87.2				X		X	X
	4	87.7	X			X		X	X
	5	88.3	X		X	X		X	X

[1]Heat degree days; [2]Hourly mean air temperature; [3]Minimum air temperature; [4]Maximum air temperature; [5]Dew point temperature; and [6]Daily mean air temperature

One of the objectives of this study was to decrease the number of variables to possible extent without compromising the overall accuracy. A study by Afzaal et al. [36] concluded

that there was no major improvement in deep learning models predictive accuracy by increasing the number of variables from 2 to 4.

2.3.2 Descriptive Statistics of Selected Input Variables

Descriptive statistics of the selected variables are given in Table 2-2. The maximum air temperature ranged between -17 and 33.5 °C for the period 2011-2017 for all sites. The highest maximum air temperature was recorded to be 33.5 ^{O}C for Summerside. The mean of maximum air temperature was in the range of 9.2-10.7 ^{O}C with high standard deviation, i.e., 10.2-10.8 °C for all sites.

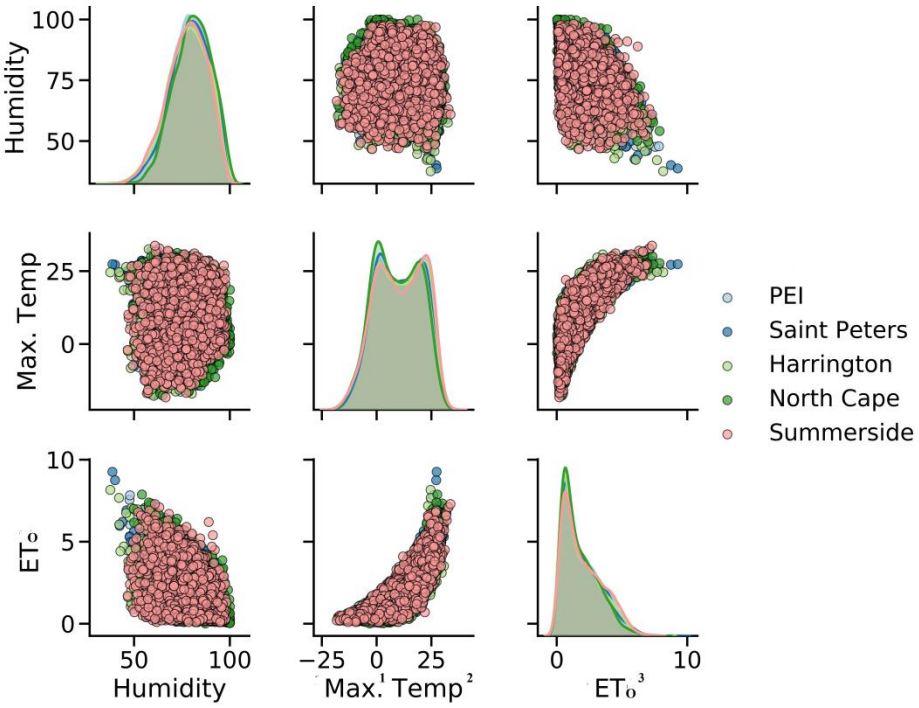

Figure 2-4 Pair plots of selected variables for year 2011-2017

Where [1]Max. Temp is Maximum air temperature; [3]ETo is reference evapotranspiration computed from FAO-56 method

Because of seasonality, the maximum air temperature behaved as bimodal distribution for all sites (Figure 2-4). Exponential relation of maximum air temperature with ET_O is evident in Figure 2-4. Relative humidity ranged from 37.6 to 100% for all sites. The average humidity was recorded to be 77.7- 80.1% with higher standard deviation of 37.6 – 49.3 % in year 2011 to 2017 for all sites (Table 2-2). Relative humidity represented with normal distribution and weaker inverse relation between ET_0 and relative humidity may be visualized in Figure 2-4.

Table 2-2 Descriptive statistics of input and output variables for year 2011 to 2017

Variable	Site	Mean ± SD	Minimum	Maximum
Maximum Temperature (^OC)	Harrington	10.5±10.6	-17.7	32.5
	North Cape	9.2±10.2	-17.6	31.2
	Prince Edward Island	10.2±10.5	-17.2	31.8
	Saint Peters	10.5±10.4	-17.0	32.0
	Summerside	10.7±10.8	-18.2	33.7
Reference Evapotranspiration (mm/day)	Harrington	1.9±1.5	0.1	8.2
	North Cape	1.8±1.4	0.0	7.9
	Prince Edward Island	1.9±1.4	0.1	7.8
	Saint Peters	1.9±1.5	0.1	9.3
	Summerside	2.0±1.5	0.1	7.3
Rainfall (mm/day)	Harrington	3.1±7.0	0.0	92.9
	North Cape	3.1±7.7	0.0	147.5
	Prince Edward Island	3.0±6.0	0.0	89.7
	Saint Peters	3.2±7.1	0.0	85.3
	Summerside	2.4±6.1	0.0	103.8
Relative Humidity (%)	Harrington	78.1±10.5	37.6	99.4
	North Cape	80.7±9.6	49.3	100.0
	Prince Edward Island	78.9±9.5	47.6	98.4
	Saint Peters	79.1±10.0	38.7	98.0
	Summerside	77.7±10.2	46.7	98.3

ET0 computed from FAO-56 method ranged between 0 and 9.3 mm/day for all sites in and duration 2011-2017. The maximum daily ETO was recorded to be 9.3 mm/day for Saint Peter site. The mean daily ET0 ranged from 1.8 to 2.0 mm/day with slightly lower standard deviation of (i.e., 1.4 - 1.5 mm/day) for all sites. Distribution of daily ET0 may be represented with right skewed distribution because of relatively low values in winter season (Figure 2-4).

The rainfall varying from 0 to 147.5 mm/day was recorded for all sites in the study period. The highest rainfall of 147.5 mm was recorded for the North Cape site. The average rainfall received by all sites was in the range of 2.4 – 3.2 mm/day with standard deviation of 6 – 7.7. mm/day. The Summerside station received relatively less rainfall in comparison with other sites (Table 2-2).

2.3.3 Model Training and Testing Evaluation

In training of RNNs, several optimizers were tested including Stochastic gradient descent, Adam, Adagrad and RMSprop. The performance of Adam remained better in comparison with other optimizers in terms of accuracy and model convergence. The better performance of Adam optimizer is in agreement the findings of Reddy et al. [37]. No major effect of increasing the number of neurons on model R^2 and RMSE was observed in training of RNNs used in this study. Similarly, no major effect of different learning rates on model R^2 and RMSE was observed e.g. 10^{-2}, 10^{-3} and 10^{-4}. Dropout effect was also tested by freezing the 10, 20, and 30% random neurons to reduce the overfitting effects in training of RNNs used in this study. However, because of data normalization of the datasets the RNNs used in study were successfully converged without over and under fitting with

approximately equal training and testing accuracies. Similar results were found in a study by Afzaal et al. [36] as no major effect of dropout was observed with normalized data. Therefore, all the RNNs used in this study were trained without introducing dropout in LSTM layers.

In training of LSTM models for Saint Peter site, training and testing losses were recorded to be 0.042 and 0.0404, respectively. Approximately equal values of training and testing losses depict the successful model convergence without overfitting. LSTM models training RMSE was recorded to be 0.497 mm/day and training R^2 was recorded to be 0.88. Similarly, the value of RMSE for testing LSTM model was recorded to be 0.46 mm/day and testing R^2 was 0.91. No major differences were observed in training and testing set accuracies when modelled with Bidirectional LSTM for Saint Peters site (Table 2-3). It is evident that with both models, there were higher testing accuracies in comparison with training accuracies maybe because in training stage usually the ANNs try to adjust their weights. Another reason could be because of unequal data points for training and testing phases. The higher numbers of data points in training stage (give number of data points) might have reduced the accuracy of RNNs during training phase.

For Harrington site, slightly higher losses and lower accuracies were observed in comparison with Saint Peters site (Table 2-3). In training of LSTM for Harrington site training and testing losses were recorded to be 0.0523 and 0.0555, respectively. Training and testing RMSE were 0.54 and 0.58, respectively for LSTM models. The respective training and testing R^2 were 0.85 and 0.86, respectively. In training of Bidirectional LSTM for Harrington site, higher training and testing accuracies were recorded in comparison with LSTM. The testing accuracy of Bidirectional LSTM was 5% higher in comparison

with LSTM for Harrington site. The advance architecture of Bidirectional LSTM might help them to attain the higher accuracies in comparison with LSTM. Furthermore, the dataset of Harrington sites showed slightly higher standard deviation in comparison with other sites selected for this study. The results suggested that the Bidirectional LSTM can achieve higher accuracy with scatter data in comparison with LSTM.

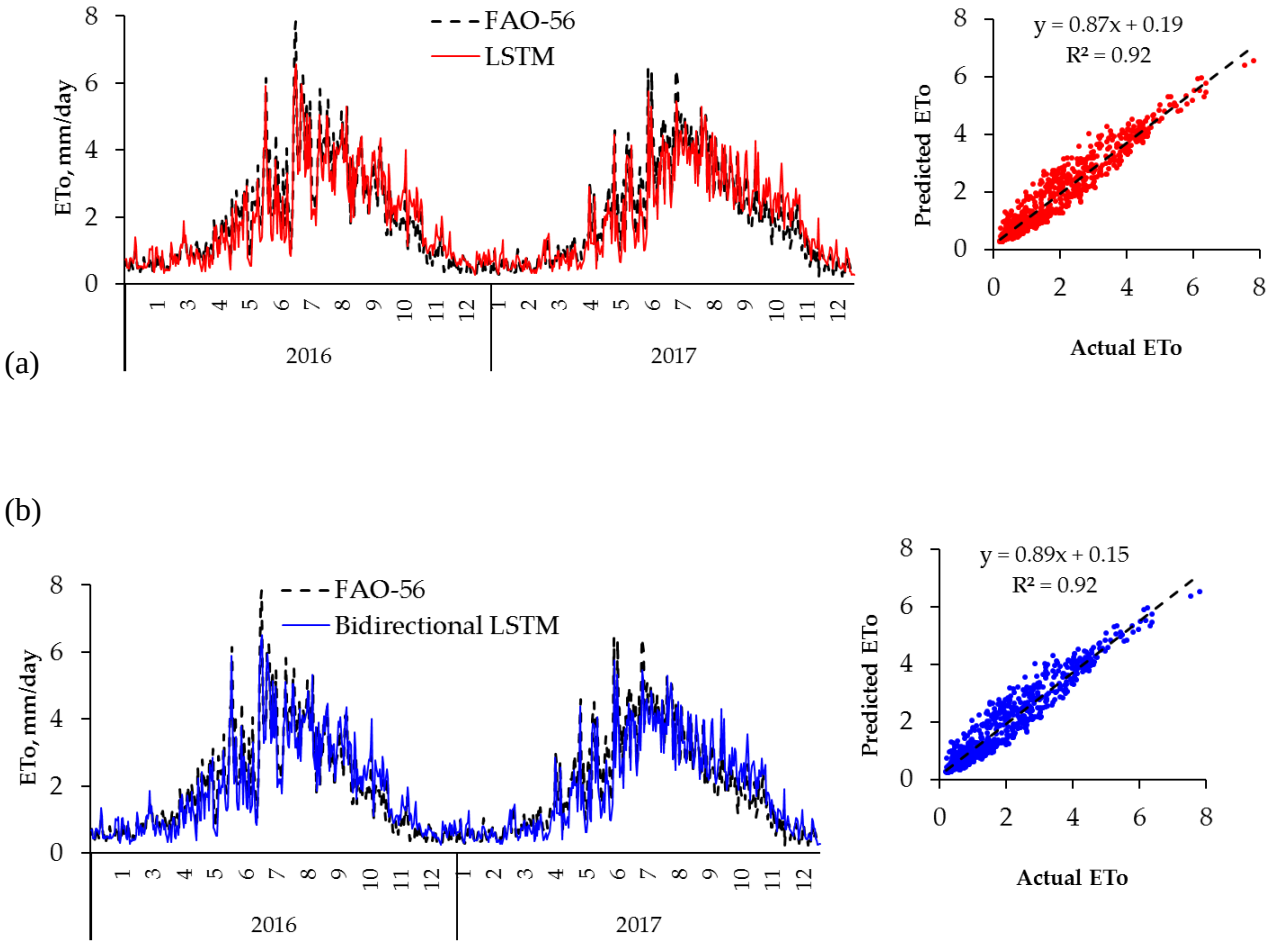

Figure 2-5 (a) Comparison of ETo predicted with LSTM and FAO-56, (b) with Bidirectional LSTM and FAO-56 using combined data set of Prince Edward Island for the test period 2016-2017

North Cape LSTM training and testing losses recorded to be 0.0337 and 0.0380 respectively, slightly lower than all other sites. The LSTM training and testing RMSE was

recorded to be 0.35 and 0.39, respectively. The LSTM training and testing R^2 was recorded to be 0.93 and 0.92, respectively. No major differences were observed in losses and accuracies for North Cape site when modelled with Bidirectional LSTM. The two directional learning may achieve the higher accuracies in time series forecasting problem. However, this study estimates the time steps of time series by inputting climatic variables only as there are no forecasting involved.

Summerside LSTM training and testing losses were recorded to be 0.0550 and 0.0490, respectively. The LSTM training and testing RMSE was recorded to be 0.53 and 0.45, respectively. The LSTM training and testing R^2 was recorded to be 0.87 and 0.91, respectively. No major differences were observed in losses and accuracies for Summerside site when modelled with Bidirectional LSTM. For both RNN, higher testing accuracies of were observed in comparison with training accuracies for Summerside.

For Prince Edward Island sight slightly lower LSTM training and testing losses were observed (Table 2-3). The LSTM training and testing R^2 were recorded to be 0.91 and 0.91 respectively. There were no major differences were observed in losses and accuracies for Prince Edward Island site when modelled with Bidirectional LSTM.

Overall, no major effect was observed in the accuracy of LSTM and Bidirectional LSTM for all sites. However, for Harrington and Prince Edward Island site the accuracy of Bidirectional LSTM was slightly better. In another similar study of turbulent flow modelling by Mohan and Gaitonde [38] who also found better performance of LSTM in comparison with Bidirectional LSTM. However, similar performance of LSTM and Bidirectional LSTM was observed except for two sites (Harrington and Prince Edward

Island; combined data) in which performance of Bidirectional LSTM was better than LSTM.

Table 2-3 Training and testing evaluation of Recurrent Neural Networks

Site	Model	Training MAE	Testing MAE	Training RMSE	Training R^2	Testing RMSE	Testing R^2
St Peters	LSTM	0.0420	0.0404	0.50	0.88	0.46	0.91
	[1]B LSTM	0.0419	0.0405	0.49	0.88	0.46	0.91
Harrington	LSTM	0.0523	0.0555	0.54	0.85	0.58	0.86
	B LSTM	0.0461	0.0450	0.48	0.86	0.46	0.91
North Cape	LSTM	0.0337	0.0380	0.35	0.93	0.39	0.92
	B LSTM	0.0340	0.0375	0.34	0.93	0.38	0.92
Summerside	LSTM	0.0550	0.0490	0.53	0.87	0.45	0.91
	B LSTM	0.0563	0.0497	0.53	0.87	0.45	0.91
Prince Edward Island	LSTM	0.0417	0.0438	0.40	0.91	0.42	0.91
	B LSTM	0.0415	0.0437	0.40	0.91	0.42	0.92

1B LSTM; Bidirectional LSTM

2.3.4 Rainfall and Reference Evapotranspiration Comparison

One of the objectives of this study was to highlight the gap between ET_0 and rainfall in order to strategize the need for supplemental irrigation and sustainable agriculture. A comparison between the cumulative values of rainfall and ET_O for the period 2011-2017 is displayed in Figure 2-6 to gauge the gap between the two variables. The results showed a high variability of rainfall in different months (of the growing season) during all years of the study period than variability in ET_O. For the month of June, the rainfall ranged between 64.85-107.025 mm while FAO-56 ET_O ranged between 83.82-112.47 mm with an average difference of 13.52 mm. The ET_0 clearly surpassed the rainfall values in month of June for periods 2011-2014 and 2016-2017. The highest gap between rainfall and ET_0 was observed in the month of July for year 2012-2017. In July the recorded difference between ET_0 and rainfall was computed to be 3.66, -92.2, -56.1, -85.0, -73.4, -68.5, -98.7 mm for years 2011

through 2017, respectively. The negative values clearly show the higher ET_0 than the respective rainfall. In month of August, the ET_0 surpassed rainfall in year 2012, 2013, 2015 2016 and 2017 by 46.1, 30.0, 4.39, 15.8, and 39.6 mm, respectively. In the month of September, October and November, rainfall clearly surpassed the ET_O. These are the months of crop harvest when crops do not need rainfall and have no ET phenomena.

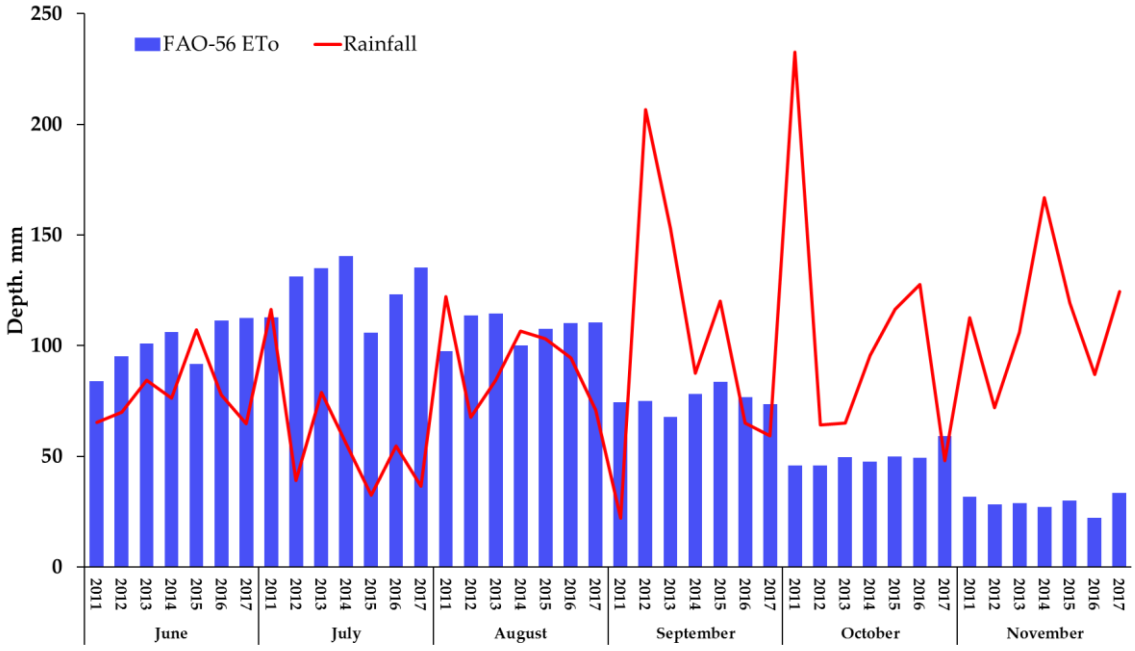

Figure 2-6 Rainfall and FAO-56 ETo comparison for the study period 2011-2017

The result of this analysis suggested that rainfall is highly variable in same months of different year unlike ET_O, which seems to be more consistent in different years. In order to fulfill the crop water requirements, careful monitoring is required in months of June, July and August in Prince Edward Island for potential crop yield.

Suitability of the modelling approach adopted in this study was further evaluated by comparing the FAO-56 cumulative ET_O with the values simulated using LSTM and Bidirectional LSTM in Figure 2-7, where cumulative rainfall has also been plotted for the

test periods 2016 and 2017. A close agreement was found between ET_O determined with FAO-56 and the two RNNs.

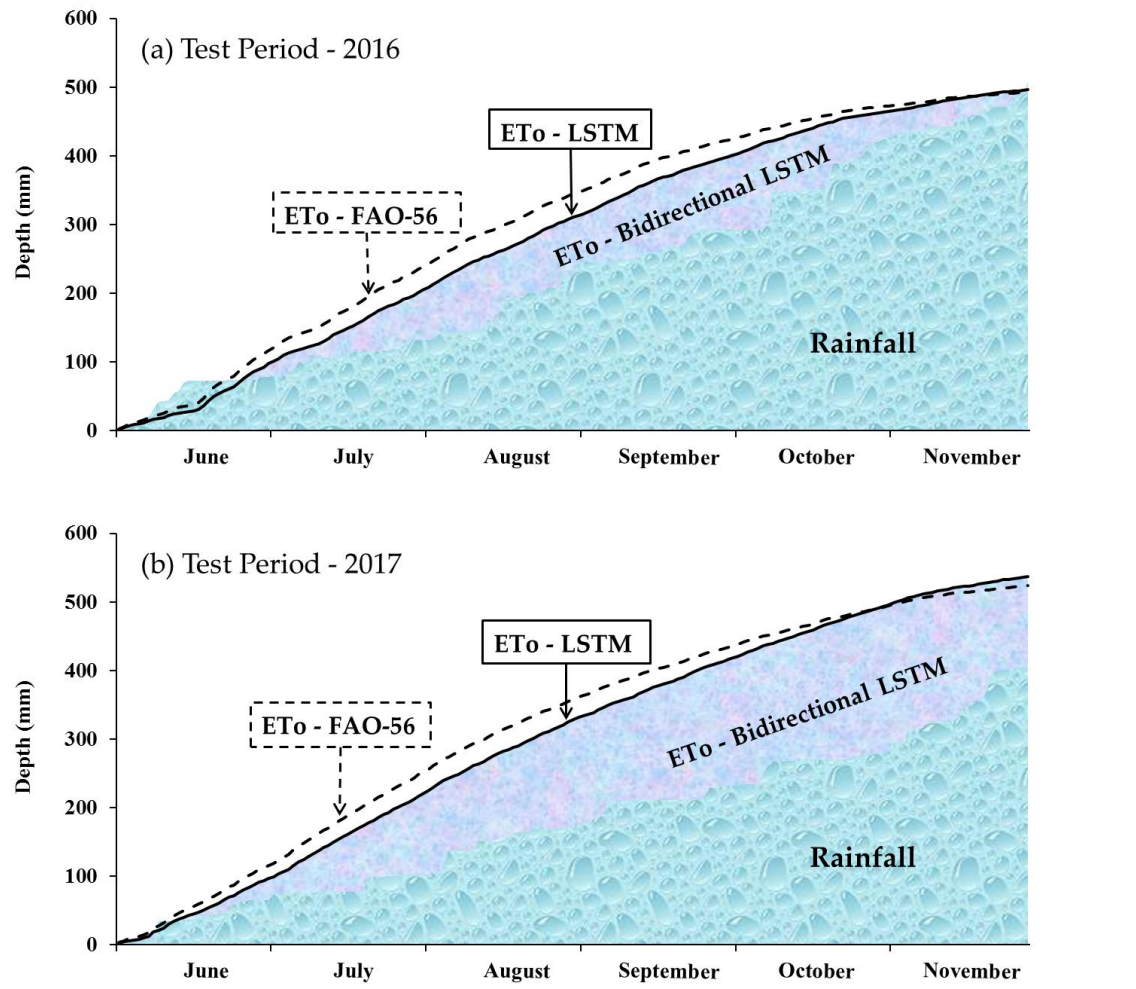

Figure 2-7 (a) Rainfall, FAO-56 ETo, LSTM ETo, Bidirectional ETo comparison (a) 2016 (b) 2017

Despite overestimation during the period July-October, yearly cumulative values of ET_O determined with all the three methods were also in good agreement with cumulative rainfall during 2016 (Figure 2-7a). During the year 2017, higher cumulative gaps were observed between ET_O and rainfall in comparison with 2016 (Figure 2-7b). The lower

rainfall during the growing season (June-November) of 2017 (403.74 mm) than during 2016 (506.69 mm) were responsible for these gaps. There was no difference in the trends of RNNs and FAO-56 ET_O for the two test years. The cumulative gaps between values of FAO-56 - ET_O and the values of ET_O determined with LSTM and Bidirectional LSTM depict the predictive errors of RNNs models. The error may be further reduced by adding more input variables in RNNs model. Furthermore, underestimations for drier months and overestimation for colder months may be removed by adding RMSE correction factors in order to obtain more accurate predictions. The results support the applicability of LSTM and Bidirectional LSTM for sustainable water management with accurate estimation of ET_O. In order to replenish the crop water requirements, supplemental irrigation might be the option for certain months of the growing season when ET_O surpassed rainfall.

2.4 Conclusions

Reference ET was estimated using LSTMs and Bidirectional LSTM at four sites of Prince Edward Island namely Saint Peters, Harrington, Summerside and North Cape for study period 2011-2017. Meteorological data were split into two sets namely training set (2011-2015) and testing set (2016-2017). Based on subset regression analysis using nine different climatic variables, maximum air temperature and relative humidity were selected as inputs for recurrent neural networks. By using tuned hyperparameters the LSTM and Bidirectional LSTM were able to estimate ET_0 with considerable accuracies determined with method of FAO-56. There were no major differences in the accuracy of LSTM and Bidirectional LSTM. However, for Harrington site, Bidirectional LSTM performed better in comparison with LSTM for testing set (2016-2017). The advance architecture of Bidirectional LSTM might be help in attaining the higher accuracies in comparison with

LSTM. Furthermore, the dataset of Harrington sites showed slightly higher standard deviation in comparison with other sites selected for this study. The results suggested that the Bidirectional LSTM can achieve higher accuracy with scatter data in comparison with LSTM. Another objective of this study was to quantify the difference ET_O and rainfall. The analysis showed that in months of June, July and August the ET_O surpassed rainfall. Viable options such as supplemental irrigation may be needed to replenish the crop water requirements in drier for agriculture sustainability.

CHAPTER 3

Precision Irrigation Strategies for Sustainable Water Budgeting

Abstract

Climate change induced uneven patterns of rainfall emphasize the use of supplemental irrigation (SI) in rainfed agriculture. The Penman-Monteith method was used to calculate SI for water budgeting of potato fields in Prince Edward Island, Canada. Cumulative gaps between rainfall and crop evapotranspiration (ETc) in August and September, due to high crop coefficient factor justified the need for SI during 2018 and 2019. Pressurized irrigation systems including sprinkler, fertigation and drip irrigation were installed to evaluate the impact of scheduled SI to offset deficit in irrigation water requirements as compared to conventional practice of rainfed cultivation (control). A two-way ANOVA examine the effect of irrigation methods and year on potato tuber yield, water productivity, tuber quality, and payout. Sprinkler and fertigation systems performed better in comparison with drip and control treatments. In term of payout returns and potato tuber quality (percentage of marketable potatoes), sprinkler treatment performed significantly better than the other treatments. However, in terms of water productivity, fertigation treatment performed significantly better than control and sprinkler treatments in both years. The use of SI is recommended for profitable cultivation of potatoes in soil, agricultural, and environmental conditions resembling to those of Prince Edward Island.

3.1 Introduction

Potato (Solanum tuberosum L.) is the world forth most important food crop [39]. The utilization of potato in human nourishment and the scratch manufacturing distinguishes it from other vital crops on the planet [40]. Potato industry significantly promotes the economy of PEI as it contributes about 10.8% to the GDP of this province with more than one billion direct and indirect economic benefits engaging 12% of total work force of the island [41]. Currently, Prince Edward Island is producing approximately 25% of total potatoes grown by Canada each year [42].

Several sstudies have been conducted to assess the effects of SI on potato tuber yield. For example, Belanger et al, [43] tested the irrigation and nitrogen fertilizers effects on two potato cultivar yield in New Brunswick Canada. Results indicated the increased potato yield from 31.9 Mg ha^{-1} to 38.4 Mg ha^{-1} and marketable yield from 25.6 Mg ha^{-1} to 30.7 Mg ha^{-1}. Similar results were recorded for both potato cultivars. Porter et al, [44] studied the soil management and supplemental irrigation effect on potato tuber yield and quality. Supplemental irrigation significantly increased total yields by 10.6 Mg ha-1 to 11.6 Mg ha-1. Similarly, potato tuber size was significantly increased from the result of supplemental irrigation, while decreased specific gravity of potato tubers was observed. Supplement irrigation largely depends upon the amount of rainfall and crop water requirements.

Evapotranspiration (ET) is major contributor in water balance as well as surface energy equation. ET provides useful information regarding irrigation quantification and efficient water resources management. Several direct and indirect methods of ET estimation have been introduced in an attempt to increase the accuracy of estimation. The choice of method solely depends upon the data availability and accuracy of estimation.

Kashyap and Panda, [45] compared the 10 different climatological methods of estimating ETo. The climatological methods were estimated using the lysimeter with electric datalogger. The result suggested that the Penman Monteith equation was the best estimation method in comparison with other methods.

Several irrigation methods have been tested previously to replenish the crop water requirements on need basis. Onder et al. [46] studied the effect of surface and sub-surface drip irrigation methods with four different water stress levels on potato yield and yield components. The four stress levels were tested including full irrigation, 66% of full irrigation, 33% of full irrigation and no irrigation. No significant differences of irrigation methods were observed on yield. However, the result depicted that the drip irrigation has several advantages over sub-surface irrigation in terms of installation and replacement costs. Water stress significantly affected the potato yield and yield components of early potato yield production. More than 33% deficiency of irrigation requirements of potato crop is not suggested. Stylianou et al. [47] evaluated the effects of sprinkler and trickle irrigation on potato yield on the basis of pan evaporation. The results suggested that the trickle irrigation was not the suitable method for potatoes as soil cracked and exposed the potato tubers to be attack by the moths. In another study by Unlu et al. [48] evaluated the effects of trickle and sprinkler irrigation in the middle Anatolian, Turkey. In this study, three irrigation methods were selected namely sprinkler, drip and fertigation. The highest yield was measured in sprinkler irrigated plots at the 60 gm-3 nitrogen concentration levels.

Prince Edward Island is surrounded by ocean from all the sides which require efficient and careful water resources management to avoid saltwater intrusion. Agriculture in Prince Edward Island is rainfed mostly; however, changing rainfall patterns due to climate change,

several high capacity wells were installed in PEI for supplemental irrigation to compensate drought periods in drier months of years. These steps have raised concerned about groundwater sustainability. A recent study by Afzaal et al. [36] pointed out the reduced groundwater levels than expected in summer season due to pumping. This situation has created the challenges for water resources manager to meet the SI demands in sustainable ways. In this study several irrigation methods had been evaluated to assess the potato tuber yield, quality, water productivity and payout returns. The results of this study will provide the guidelines to water resource managers for sustainable water management. There has been limited work in literature for Prince Edward Island region, which make this work novel and useful for potato growers as well as policy makers.

3.2 Materials and Methods

3.2.1 Study Field, Experimental Design, and Soil Properties

The experiments reported here were conducted on a research farm at Kensington, Prince Edward Island (46.417032 ^{0} N 63.67658 ^{0} W). The field of 1003.35 m^2 was divided in four treatments namely sprinkler, drip, fertigation and control triplicated on 41.8 m^2 plots (Figure 3-1). Patches of 3 m were left between treatment plots to serve as buffer zones and walkways for data collection, agronomic operation, field management activities. The experiments were under complete randomized design with two factorial arrangements. The irrigation methods and the growing years were the two independent factors with continuous response variables including potato tuber yield, tuber quality, water productivity and payout (Figure 3-1).

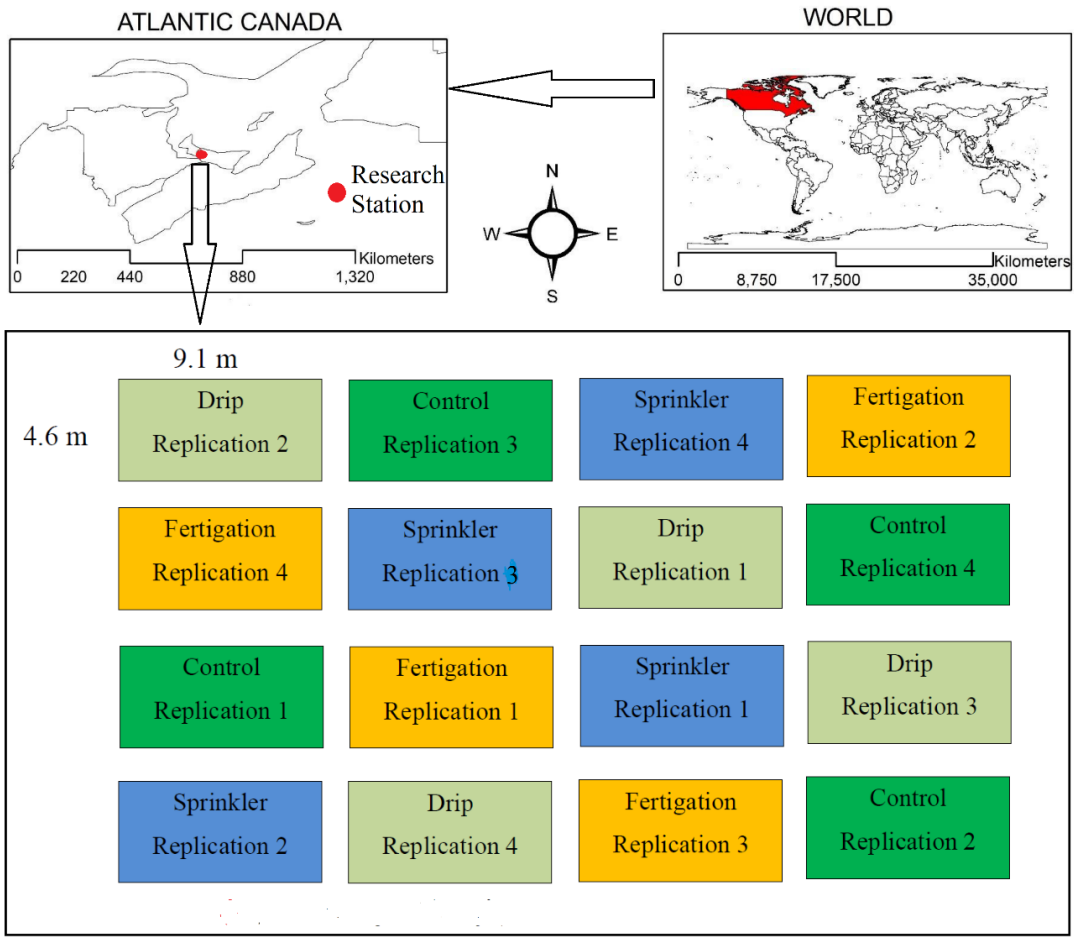

Figure 3-1 The location of experimental field and experimental layout

Two soil samples were collected from each replication and homogenized prior to their analyses for soil macro- (nitrogen, N; phosphorous, P; and potassium, K), micro-nutrients (boron, B; copper, Cu; zinc, Zn; magnesium, Mg; iron, Fe; calcium, Ca), organic matter, and soil pH. Soil analyses were conducted by Prince Edward Island Analytical Laboratories with standard methods. Soil analysis results (Table 3-1) were used to determine crop nutrient requirement.

Table 3-1 Descriptive statistics of soil variables

Variable	Irrigation Methods	Mean± SD	Minimum	Maximum
Organic Matter %	Control	2.9±0.30	2.50	3.40
	Drip	2.8±0.18	2.50	3.10
	Fertigation	2.8±0.28	2.50	3.40
	Sprinkler	2.8±0.23	2.50	3.00
Phosphate (mg/kg)	Control	490±47.4	401	548
	Drip	456±46.9	378	513
	Fertigation	488±43.1	402	541
	Sprinkler	459±49.0	383	519
Phosphorous (mg/kg)	Control	135.0±0	135	135
	Drip	135.0±0	135	135
	Fertigation	135.0±0	135	135
	Sprinkler	135.0±0	135	135
Potash (mg/kg)	Control	182±19.1	151	213
	Drip	147±15.3	115	168
	Fertigation	157±12.9	142	179
	Sprinkler	152±15.6	128	166
Copper (mg/kg)	Control	0.42±0.07	0.40	0.60
	Drip	0.45±0.07	0.40	0.60
	Fertigation	0.42±0.07	0.40	0.60
	Sprinkler	0.45±0.07	0.40	0.60
Soil pH	Control	6.60±0.05	6.50	6.70
	Drip	6.64±0.05	6.60	6.70
	Fertigation	6.59±0.06	6.50	6.70
	Sprinkler	6.73±0.04	6.70	6.80
CEC (meq/100g)	Control	9.37±0.51	9.00	10.0
	Drip	8.87±0.64	8.00	10.0
	Fertigation	9.50±0.53	9.00	10.0
	Sprinkler	7.80±0.30	7.00	8.00

3.2.2 Crop Water Requirements

Penman-Monteith method was used to estimate the ET_C, which is integral part of soil water balance equation expressed as [49][50] may express as:

$$P = Q + ET_c + \Delta S \qquad (3-1)$$

where P is precipitation; Q is runoff; and ΔS is change in soil moisture storage. ET_C is crop evapotranspiration, which is calculated with the relationship involving crop coefficient factor (k_C) and ET_O [21]:

$$\mathrm{ETc} = \mathrm{ETo} * \ \mathrm{kc} \qquad (3-2)$$

The ETo is calculated as:

$$\mathrm{ETo}\left(\frac{mm}{day}\right) = \frac{\Delta(R_n - G) + \rho_a c_p \left(\frac{es - ea}{ra}\right)}{\Delta + \gamma\left(1 + \frac{r_s}{r_a}\right)} \qquad (3-3)$$

where, ETo = reference evapotranspiration; Δ = slope of vapor saturation pressure; R_n = net radiation; G = soil heat flux; ρ_a= mean air density at constant air pressure; c_p= specific heat of the air; *es* – *ea* = vapor pressure deficit; γ = psychrometric constant; r_s = surface resistance; r_a= aerodynamic resistance

The crop factor depends on the crop growth stage and variates among different growth stages. Potato growth stages may divide into initial (20 days after planting; DAP), development (21-50 DAP), mid (51-110 DAP) and late stage (111-140 DAP) [51]. In initial potato stage, the value of k_C fluctuates between 0.4-0.5, in development stage k_C varies between 0.7-0.8, in mid stage k_c ranges between 1.05-1.2 and in the late season k_c varies between 0.7-0.75 [51].

The water productivity (kg/m^3; kg of crop yield / m^3 of total water available to the crop) is a well-known parameter to assess the effectiveness of irrigation systems in consideration with sustainable use of water and is calculated as [52]:

$$\text{Water Productivity} = \frac{\mathrm{Ya}}{\mathrm{P} + \mathrm{I} + \Delta\mathrm{S}} \qquad (3-4)$$

where, Ya = Actual yield (kg); P = Precipitation (m^3); I = Applied irrigation (m^3); ΔS = Difference in soil water storage between planting and harvesting (m^3).

Furthermore, for the whole cropping year the filed capacity depletion level was maintained at 40%. The recommended depletion levels for potato crops are suggested to be 30-50% of soil field capacity [53][3].

3.2.3 Irrigation Methods

Three irrigation methods namely sprinkler, drip and fertigation were used to evaluate the effects of potato tuber yield. All three irrigation systems were installed using a series of piping networks with variable rate pressure pumps and water tank. The designing of pumps and tanks was based on the gaps between ETo and rainfall calculated for the period 2011-2017. Equation of continuity (Equation 5) was used to determine the pipe diameters for the irrigation systems as:

$$\mathrm{Q} = A * \mathrm{V} \qquad (3-5)$$

where, Q is flow in m^3/sec; *A* is area in m^2; V is velocity in m/sec.

Sprinkler irrigation system was designed for four replications, while the sprinkler guns were connected with 38.1 mm polyvinyl chloride (PVC) pipe. Small spray heads (Rain Bird Model 1812PRS 1800 Series) were used in conjunction with 0.3 m extension to ensure the sprinkler height with respect to maximum height of potato plants. Rain Bird adjustable arc spray nozzles (Model 10VAN) with range of 3 m were used with overlapping setups. Five spray heads were used in one replication with 70% overlap of wetting pattern radius. Pressure and flow calibrations were conducted in laboratory prior to installation of the system in experimental plots.

Drip irrigation system comprised 12.7 mm poly drip tubing with pressure compensating emitters (Model IDROP-10 4 LPH) inserted in the drip tubes based on plant to plant distances within a row. Laboratory calibrations for flow tests were conducted for the nearest and the farthest drip emitters, from the pressure pump, in order to ensure equitable flow and pressures in emitters and drip lines. Four lines of poly drip tubing were installed for one replication with 45 emitters in each line. All drip lines were connected by 19.05 mm diameter PVC pipes. Different pipe sizes were used for sprinkler, drip and fertigation system to ensure the equitable and laminar flow in pipes of different interconnected irrigation systems. In the Fertigation system, fertigation tanks (Model EZFLO-2005-HB 3/4 Gallon) were added for liquid fertilizer application with similar design as in drip irrigation system.

3.2.4 Crop Nutrient Requirements and Husbandry

Pre-sowing soil analysis results (Table 3-1) were used to calculate nitrogen phosphate and potassium (NPK) application rates for the experimental treatments by following the nutrient recommendations from Prince Edward Island Department of Agriculture and Fisheries [24]. Because of no substantial variations between NPK concentrations among the experimental treatment plots during both years, almost the same application rates were calculated and used for the respective treatments. Except in fertigation treatment plots, the NPK were applied with broadcasting method that refers to uniform spreading of granular fertilizer over the soil surface in contrast of localized application of fertilizer that refers to spreading fertilizer in a band or a circle near around the seed/field furrows or plants. In the rest of the treatments, respectively 160, 135, and 135 kg/ha of N, P, and K were applied at

the time of sowing and on July 28, 2018 and respectively 180, 135, and 135 kg/ha of N, P, and K were applied at the time of sowing and on July 25, 2019. In the fertigation treatment plots, one-third of the NPK application rates were applied on three separate occasions i.e., on sowing, July 15 and July 31 during 2018 growing season and on sowing, July 20 and July 29 during 2019 growing season. Seed potatoes (Russet Burbank) were sown on June 11, 2018 and on June 10, 2019 for the two respective growing seasons, at 0.3 m wide beds with plant to plant distance of 0.4 m and bed to bed center distance of 0.3 m. The rest of crop husbandry operations including maintenance of seed beds/furrows and weeding were done similarly in all treatment plots.

3.2.5 Data Collection

Soil moisture levels were recorded with TDR probes (Field Scout 350) at 0, 0.15, and 0.30 m soil depths each week during both planting years. Weather data were collected from Summerside (46.441111 ^{O}N 63.838056 ^{O}W) weather station for daily ETo calculations. SI was scheduled to replenish weekly transpired water from plants. Potato yield samples were collected on October 19, 2018 and October 10, 2019) from one out of 4 randomly selected rows and weighed using electronic balance with precision of 1.00 g for different quality parameters such as good-sized/marketable potatoes that were used to calculate total payout per hectare. Potatoes passing through 50-80 mm diameter holes of potato sorter were considered to be of good sized and/or marketable.

3.2.6 Statistical Analysis

Two-way analysis of variance (ANOVA) with replication method was used to evaluate the differences of mean in treatments. The statistical model used in this study may define as:

$$X_{ijk} = \mu_{ij} + \varepsilon_{ijk} = \mu + \alpha_i + \beta_j + \gamma_{ij} + \varepsilon_{ijk} \quad (3-6)$$

where X_{ijk} is estimation of model; μ_{ij} = mean of i,j group; μ=overall mean; α_i = main effects of ith row group; β_j=main effects of jth column group; γ_{ij}=interaction effect of ijth group; ε_{ijk}=errors

ANOVA assumptions such as independent observations, normal distribution, homoscedasticity within groups were evaluated for each hypothesis. ANOVA only test weather is there any significant differences in means of treatment groups or not. It does not tell which group performed better than other. For further comparison after significance, multiple mean comparison analysis is for further means comparisons. In this study, group means were tested with Tukeys pairwise comparisons test which may describe as follows:

$$\text{HSD} = \frac{M_i - M_j}{\sqrt{\frac{MS_w}{n}}} \quad (3-7)$$

Where HSD = Honest significant difference; $M_i - M_j$ = Difference of pairs of means; MS_w = Mean square with group; n= Number in treatments

3.3 Results and Discussion

3.3.1 Descriptive Statistics of Potato Yield and Components

In 2018, the highest potato tuber yield was observed for sprinkler irrigation system, i.e., 38327 kg/ha in comparison with other irrigation methods with slightly higher standard deviation of 1096 kg/ha. In 2019, 12.1% lower yield was observed for control treatment in comparison with year 2018. No major differences were observed for fertigation and drip treatment yields in 2018 and 2019. In 2019, relatively less rainfall was recorded than in year 2018, which might had caused lower yield for control treatment. The residual analysis

of potato tuber yield data suggested the applicability of ANOVA method, e.g., normal distribution, equal variance, and independent observation.

Table 3-2 Descriptive statistics of potato tuber yield and quality data for the four experimental treatments

Year	Response variable	Irrigation Method	Mean ± SD	Minimum	Maximum
2018	Yield (kg/ha)	Control	35493 ± 408**a**	34889	35782
		Drip	35317 ± 820**a**	34130	35943
		Fertigation	36983 ± 667**a**	36119	37645
		Sprinkler	38327 ± 1096**a**	37173	39744
	Marketable potatoes (%)	Control	52.8 ± 5.40	45.3	58.2
		Drip	55.5 ± 2.60	52.9	59.0
		Fertigation	55.0 ± 1.20	53.3	56.0
		Sprinkler	64.3 ± 2.00	61.3	65.8
2019	Yield (kg/ha)	Control	30939 ± 1673**b**	28682	32268
		Drip	35305 ± 1975**a**	32820	37470
		Fertigation	36686 ± 1272**a**	34989	38072
		Sprinkler	34413 ± 3407**ab**	31826	38273
	Marketable potatoes (%)	Control	69.1 ± 11.5	52.5	77.7
		Drip	80.6 ± 1.20	79.8	82.4
		Fertigation	74.4 ± 6.70	70.0	84.3
		Sprinkler	82.2 ± 3.20	79.2	85.7

Different letters in the same columns indicates significant statistical differences ($p < 0.05$, Tukey's test)

Overall, higher percentages of marketable potatoes were recorded in year 2019 in comparison with year 2018 (Table 3-2). For example, the highest percentages of marketable potatoes were recorded for sprinkler irrigation system for 2019 (82.2%) in comparison with year 2018 (64.3%). The lowest percentages of marketable potatoes were recorded for control treatment in both years indicating that the irrigation played important role during tuber development stages. Furthermore, the residual analysis of marketable potatoes data suggested the applicability of ANOVA method.

3.3.2 Gaps between Rainfall and Evapotranspiration

There was substantial variability in rainfall and ETo for different months of a potato growing season (June-October) during 2011-2017 (Figure 3-2) – a period considered i) by Penman-Monteith method for estimation of ETo and ii) for requirement of water for irrigation systems, pipe diameters, and the size of pump and tank used in this study. The ETo surpassed the rainfall in the month of June for years 2011-2014 and 2016-2017, and the highest gap between rainfall and ETo was observed in the month of July for year 2012-2017. In July the recorded difference between ETo and rainfall were computed to be 3.655, -92.175, -56.12, -84.96, -73.40, -68.51, -98.69 mm for years 2011 through 2017, respectively. June and July are the months of plant growth and thus irrigation needs. Less available rains during these month cause drought conditions for potato fields that adversely affect tuber yield if no SI is scheduled and applied. The negative values indicate the higher values of ETo then rainfall. In the month of August, ETo surpassed rainfall in year 2012, 2013, 2015, 2016 and 2017 by 46.08, 29.97, 4.39, 15.83, and 39.64 mm, respectively. In the months of September, October, and November rainfall surpassed ETo reflecting the availability of water when the potato fields needed irrigation.

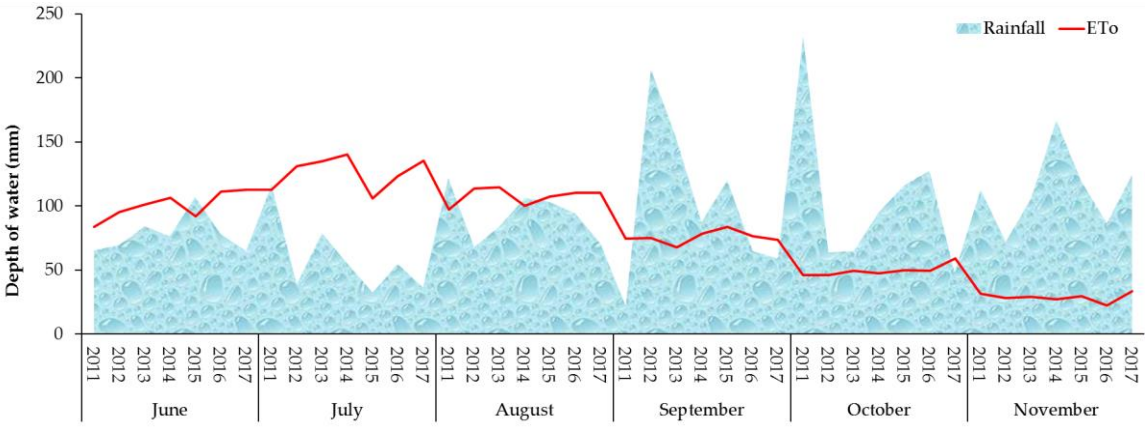

Figure 3-2 Comparison of rainfall with reference evapotranspiration for the period 2011-2017

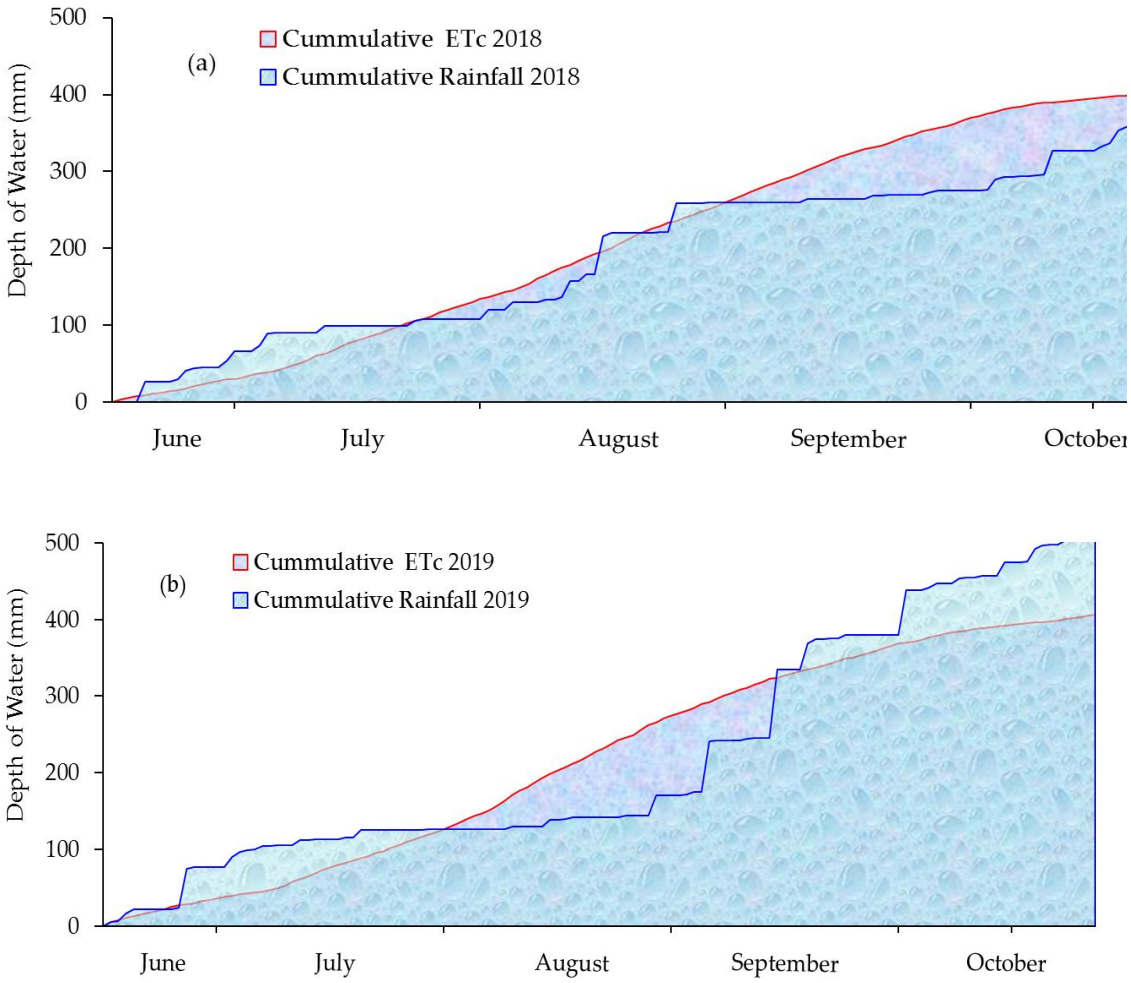

Figure 3-3 Comparison of rainfall with crop evapotranspiration for years (a) 2018 and (b) 2019

The data of ETo provided useful information in water management for larger areas; however, for irrigation scheduling of specific crop, ET_C is required. The potato crop cumulative ET_C is presented in Figure 3 for whole the cropping years of 2018 and 2019. Major differences were observed between ETo and rainfall in the months of June, July and August (Figure 3-2); however, the differences between ET_C and rainfall were minor (Figure 3-3a) in months of July, August and September 2018 due to low kc factor during initial growth stages of the potato plants. Plants require less water in their initial stages followed by increased demand of water in later stages. Due to higher kc factor (1.20) in mid potato

stages, higher differences were recorded between ET_C and rainfall in months of September and October 2018.

In the cropping year 2019, relatively less amount of rainfall occurred during the months of July and August as compared to 2018. During the growing season of 2019, the gaps between rainfall and ETc were substantial in the months of August and September. In the month of October, crop water requirements were fulfilled, and no supplemental irrigation was required.

3.3.3 Soil Water Balance

Water budgeting for an agricultural field provides useful information for irrigation monitoring, irrigation scheduling and water resource management. Information about components of water budget for the experimental fields is displayed for cropping year 2018 (Figure 3-4a) and 2019 (Figure 3-4b). During 2018, no irrigation was applied till mid-July as crop water requirements were fulfilled through rainfall. In July, one supplemental irrigation was applied to maintain the 40% depletion of field capacity in soil.

In July, several rainfall events occurred to replenish the crop water requirements. Three irrigation events were applied in the month of September 2018, which was relatively a drier month as compared to other months of the study period. Frequent rainfall events fulfilled the crop water requirements making saturation in soil close to its field capacity for several days of October 2018 (Figure 3-4a). In 2019, frequent rainfall events in the months of June, July, September, and October satisfied the crop water needs and required no supplemental irrigation. In 2019, relatively less rainfall events occurred in the months of June, July, and August. However, no irrigation was applied till mid-July 2019 because of

relatively low water needs by potato crop in its initial stage as well as at least 40% maintained depletion levels of soil field capacity.

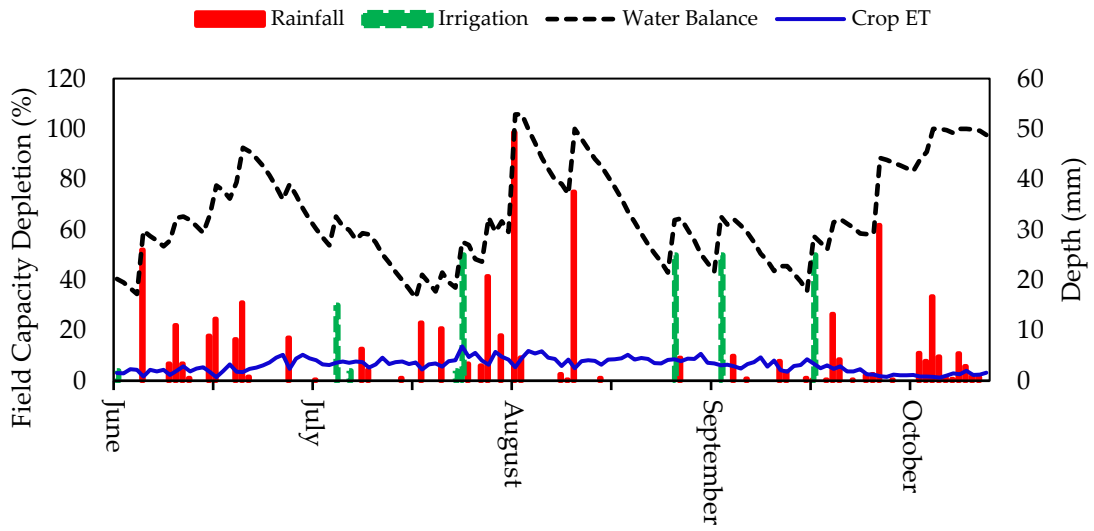

(a)

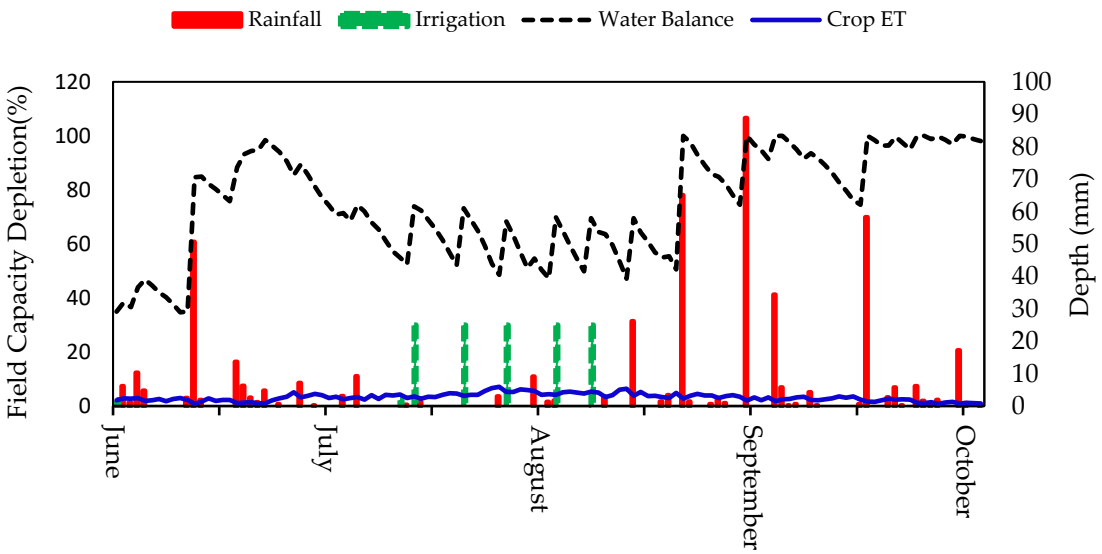

(b)

Figure 3-4 Budgeting of water for the experimental fields using water data for years (a) 2018 and (b) 2019

Five irrigations of the calculated depths were applied in late July and three weeks of August to maintain the desired moisture levels in soil (Figure 3-4b). From late August to October 2019, three heavy rainfall events occurred (> 50 mm) and helped fulfilling potato crop's irrigation water requirements or consumptive use.

3.3.4 Water Productivity

The Figure 3-5 represents the water productivities for different irrigation systems in years 2018 and 2019. In 2018, the highest water productivity (e.g., 1.4174 kg/m^3) was recorded for fertigation system in comparison with other irrigation methods. The lowest water productivity was recorded for sprinkler irrigation system as this system consumed 6.8 times more water than drip and fertigation system. The water productivity of drip irrigation system was less than control treatment; i.e., 1.35 kg/m^3. The non-uniform germination of potato plants in drip replication plots and the resultant asymmetrical alignment of drip emitters with potato plants in 2018 might be the cause of low water productivity for drip irrigation system during this year.

In 2019, similar trend of previous year was observed for fertigation and sprinkler irrigation systems; e.g., the highest (1.53 kg/m^3) and the lowest (1.19 kg/m^3) water productivities for these treatments, respectively. In 2019, higher water productivity (1.47 kg/m^3) was observed for drip irrigation system in comparison with year 2018 (1.35 kg/m^3) as the alignments of drip emitters were adjusted with growth of potato plants. This can be recommended as one of the best management practices and/or techniques for efficient potato cultivation under drip irrigation system.

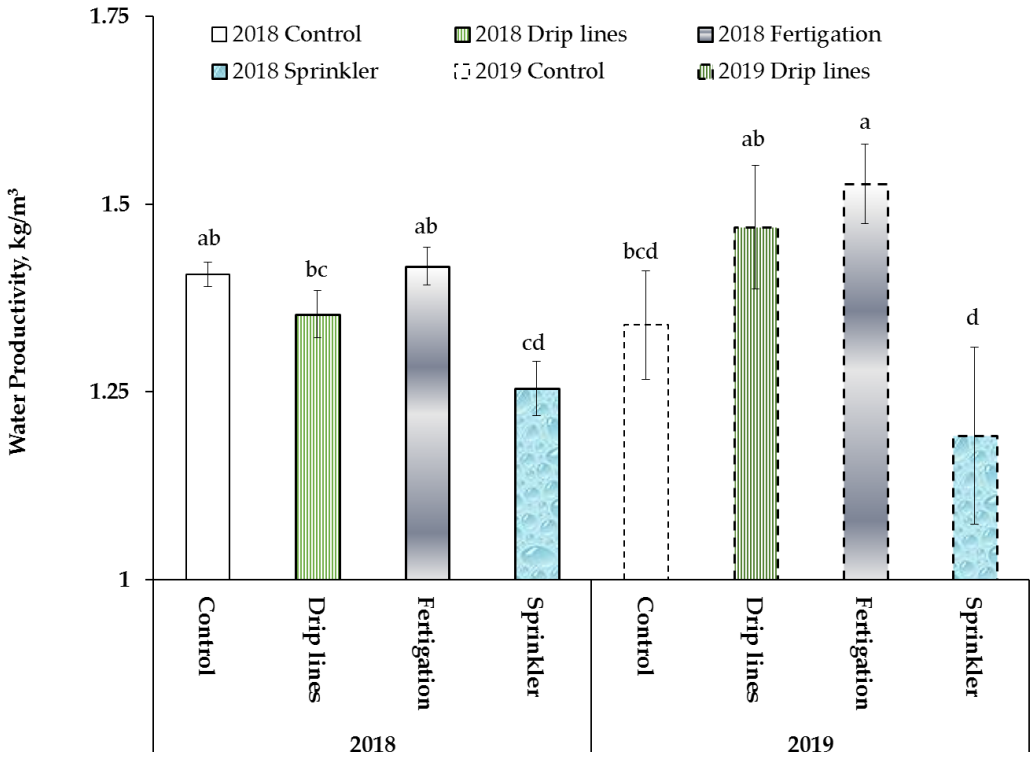

Figure 3-5 Water productivities for different irrigation systems in 2018 and 2019

3.3.5 Payout Returns

In 2018, the highest payouts per hectare were calculated for sprinkler irrigation system, e.g., \$6786.7 ha^{-1} (Figure 3-6). The highest percentages of marketable potatoes were the major reason for higher financial gains for the sprinkler irrigation system. Instead of the lowest potato tuber yield in case of drip irrigation system in 2018, the mean payout was \$211.1 ha^{-1} higher than control treatment. The higher payout for drip irrigation system indicated that the timely irrigation impacted the potato tuber development and quality.

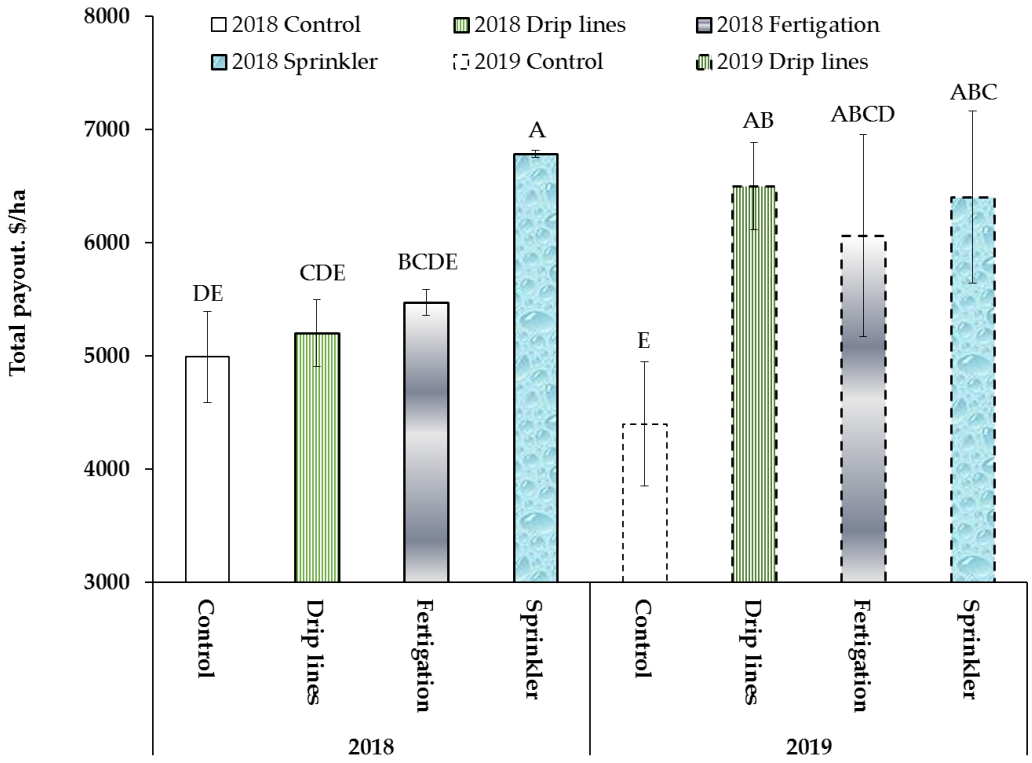

Figure 3-6 Payout per hectare for different irrigation systems in 2018 and 2019

Similarly, higher payout was recorded for fertigation system also in 2018; e.g., \$5227.1 ha^{-1}. In 2019, the highest financial gain was attained by the drip irrigation system, e.g., \$6503.95 CAD ha^{-1}, which was \$2104.55 CAD ha^{-1} higher than control treatment. Similarly, sprinkler and fertigation treatments earned \$6062.77 ha^{1} and \$6408.8 CAD ha^{-1} respectively, which were \$237.77 CAD ha^{-1} and \$329.9 CAD ha^{-1} higher than control treatment, respectively (Figure 3-6).

3.3.6 Effects of Irrigation Methods and Years

A two-way ANOVA was run to examine the effects of irrigation methods and year on potato tuber yield and quality. There was a significant interaction (Irrigation method x Year) on potato tuber yield, $F(3, 23) = 4.54$, $p = 0.012$, indicating at least one statistically

different irrigation method x year combination. Simple main effects analysis showed that there was a significant effect of irrigation methods and year on potato tuber yield (Table 3-3). However, in case of significant interaction, it is advisable to consider the interactions effect only by ignoring the main effects. Table 3-3 represents all the possible combination of irrigation method and year combinations.

Table 3-3 Two way analysis of variance table for statistical comparison

Response Variable	Sources	Degree of Freedom	Mean Squares	F-Value	P-Value
Potato tuber yield (kg/ha)	Year	1	36955884	15.3	0.001
	Irrigation Methods	3	20380293	8.43	0.001
	Year*Irrigation Methods	3	10966955	4.54	0.012
	Error	23	2417954		
	Total	30			
Good sized potatoes (%)	Year	1	2975.95	100	0
	Irrigation Methods	3	202.35	6.80	0.002
	Year*Irrigation Methods	3	28.96	0.97	0.422
	Error	23	29.74		
	Total	30			
Total payout per hectare (Dollars)	Year	1	163220	1.66	0.211
	Irrigation Methods	3	1859110.23	19.0	0
	Year*Irrigation Methods	3	612896.7	6.23	0.003
	Error	23	98435.5		
	Total	30			
Water Productivity (kg/m^3)	Year	1	0.004427	1.24	0.276
	Irrigation Methods	3	0.081653	23.0	0
	Year*Irrigation Methods	3	0.020386	5.73	0.004
	Error	23	0.003557		
	Total	30			

Several ‘irrigation method x year’ combinations were found to be significant. There were no significant differences observed between irrigation methods and control treatment in 2018. However, several treatments of 2018 were significantly different with 2019 treatments. For example, potato tuber yield in 2018 for control treatment was significantly higher than in 2019. The lower amount of rainfall in months of July and August in 2019 justifies the lower potato tuber yield for control treatment. Contrary to control treatment, sprinkler irrigation system yield was significantly higher in 2018 than 2019. Potato tuber yield of sprinkler-2019, fertigation-2019, drip-2019 was significantly higher than control-2018. Similarly, potato tuber yield of Fertigation-2018, drip 2019 was significantly higher than control-2019 (Table 3-3). The results suggested that the sprinkler irrigation system performed better in 2018 and fertigation systems performance was better in 2019. However, based on statistical analysis, no irrigation system performed consistently better in the two consecutive years to give a higher potato tuber yield.

Results of the two-way ANOVA to examine the effects of irrigation methods and year on potato tuber quality suggested a non-significant interaction (Irrigation method x year) $F(3, 23) = 0.97$, $p = 0.422$. Simple main effects analysis showed that there was a significant effect of irrigation methods on potato quality $F(3, 23) = 6.80$, $p = 0.002$ indicating that at least one irrigation method performed significantly different than other irrigation methods. Further analysis suggested that the sprinkler and fertigation systems yielded higher percentages of marketable potatoes than control treatment. However, no significant differences were observed between drip and control treatments. Similarly, no significant differences were observed between sprinkler and fertigation systems. Main effect analysis also showed that there was a significant effect of year on potato quality $F(3, 23) = 100$, p

= 0.0 indicating that in one year irrigation method yielded better quality potatoes than in the other year. Further analysis of multiple means comparison suggested that the in year 2019 the percentages of marketable potatoes was significantly higher than 2018.

A significant interaction (Irrigation method x year) on payout returns was observed, $F(3, 23) = 6.23$, $p = 0.003$, indicating at least one statistically different 'irrigation method x year' combination. In 2018, sprinkler payout returns were significantly higher than drip, fertigation and control treatments. However, no significant differences of payout returns were observed between control, drip and fertigation treatments in 2018. The higher payout returns of sprinkler irrigation system were due to higher percentages of marketable potatoes yielded from this treatment. Furthermore, all the irrigation methods had the significantly higher payout returns than the control treatment in 2019. However, no statistical differences of payout returns were observed between sprinkler, drip and fertigation treatments in 2019 (Table 3-3).

A similar significant interaction (Irrigation method x year) on water productivity was observed as for payout returns and tuber yield; e.g., $F = (3, 23) = 5.73$, $p = 0.004$. The water productivity of fertigation in 2018 was significantly higher than control and sprinkler irrigation system. The main reason behind higher water productivity of fertigation treatment was the lower water consumption as well as higher yield in comparison with control and sprinkler treatments. No significant differences were observed between sprinkler and drip treatments in 2018. Similar consistent trend was observed in 2019 for fertigation treatment; e.g., significant higher water productivity than sprinkler and control treatments. Due to similar trend of treatment in both years; there was non-significant effect of year was recorded (Table 3-3).

3. 4 **Conclusions**

This study evaluates the benefits of using irrigation scheduling and SI for sustainable irrigation water management in potato fields. The Penman-Monteith modified method was used to test whether the rainfall is enough for sustainable potato production in Prince Edward Island or SI is needed in addition to rainfall. The result highlighted the cumulative gaps between rainfall and crop evapotranspiration (ETc) in months of August and September due to higher value (kc > 1) of crop development factor requiring higher amounts of water in year 2018 and 2019. Pressurized irrigation systems including sprinkler, fertigation and drip irrigation were installed to evaluate the impact of scheduled SI to offset deficit in irrigation as compared to conventional practice of rain-fed conditions; i.e., no irrigation practice (control). A two-way ANOVA examined the effect of irrigation methods and year on potato tuber yield, water productivity, payout returns and potato quality. The samples were collected in year 2018 and 2019 potato growing seasons. A significant interaction (irrigation methods x year) was recorded on potato tuber yield, $F(3, 24) = 4.54$, $p = 0.012$ indicating at least one significantly different combination than other. Sprinkler and fertigation system performed better in year 2018 and 2019, respectively in comparison with other irrigation methods. In term of payout returns and potato tuber quality (percentage of marketable potatoes); sprinkler irrigation treatment performed significantly better than control, drip and fertigation treatments. However, in terms of water productivity; fertigation system performed significantly better than control and sprinkler treatments in both years. This study evaluated the three irrigation methods in consideration with different aspects; e.g. raw tuber yield, tuber quality, payout returns and water sustainability. It is concluded that the choice of irrigation methods largely depends on the

geographical factors influencing water availability, farm returns and applications for which potatoes are planned to be grown; i.e., for home use or marketing.

CHAPTER 4

Groundwater Estimation from Major Physical Hydrology Components Using Artificial Neural Networks and Deep Learning

Abstract

Precise estimation of physical hydrology components including groundwater levels (GWLs) is a challenging task, especially in relatively non-contiguous watersheds. This study estimates GWLs with deep learning and artificial neural networks, namely a multilayer perceptron, long short term memory, and a convolutional neural network with four different input variable combinations for two watersheds (Baltic River and Long Creek) in Prince Edward Island, Canada. Variables including stream level, stream flow, precipitation, relative humidity, mean temperature, evapotranspiration, heat degree days, dew point temperature, and evapotranspiration for the 2011–2017 period were used as input variables. Using a hit and trial approach and various hyperparameters, all artificial neural networks were trained from scratched (2011–2015) and validated (2016–2017). The stream level was the major contributor to GWL fluctuation for the Baltic River and Long Creek watersheds (R^2 = 0.51 and 0.49, respectively). The multilayer perceptron performed better in validation for Baltic River and Long Creek watersheds (RMSE = 0.471 and 1.15, respectively). Increased number of variables from 1 to 4 improved the RMSE for the Baltic River watershed by 11% and for the Long Creek watershed by 1.6%. The deep learning techniques introduced in this study to estimate GWL fluctuations are convenient and accurate as compared to collection of periodic dips based on the groundwater monitoring wells for groundwater inventory control and management.

4.1 Introduction

Groundwater is the major source of industrial and potable water supplies in Prince Edward Island, Canada [54]. Over the past few years, there has been increased demand in the agriculture sector for supplemental irrigation, which poses several challenges for water and resource managers. Because of the relatively small and non-contiguous watersheds in Prince Edward Island, pumping groundwater has also raised concerns for groundwater sustainability due to the island's uneven topography [8]. An inventory of groundwater is necessary for efficient water resource management, especially in relation to growing groundwater demands for agricultural use. It is neither feasible nor economical to install and manage monitoring groundwater wells in a place like Prince Edward Island, which consists of 260 watersheds for efficient water management. The inventory control of the groundwater resource can ensure the sustainability of water resources in the areas where groundwater pumping is common for supplemental irrigation or for domestic use.

Groundwater level (GWL) modeling provides useful information to water resource managers, engineers, and policy makers to make appropriate decisions. The modeling of GWLs is a complicated procedure that requires thorough knowledge of physical hydrological parameters, big data, hydrological models, model inputs, and the geometry of watersheds [55]. Aspects of hydrogeology—i.e., geological factors affecting the distribution and movement of groundwater underneath the soil surface—need to be properly understood when modeling GWLs and manipulating the modeling results. Watershed scale fluctuations in GWLs occur over a period of several decades, and the resulting cumulative effects on streamflow depletion may not be fully realized for years [56]. Resultantly, depending upon the distance of the pumping station from the stream and

the geologic characteristics of the aquifer, the groundwater system may take decades to recover from streamflow depletion caused by intermittent pumping. Components of the surface—and the sub-surface physical hydrology of a watershed—i.e., streamflow and groundwater flow, respectively—are interconnected, making the stream–aquifer interaction one of the key processes governing the groundwater flow pattern in a watershed [54]. Groundwater fluctuations affect streamflow and vice versa, as the pumping wells capture groundwater that would otherwise discharge to connected streams, rivers, and other surface-water bodies [56]. Francis [57] reported that, in typical watersheds of Prince Edward Island, the base flow represents almost 80% of the streamflow in the late summer and fall months. Stream length in these island watersheds ranges from less than 1 km to 20 km. Stream widths vary from less than 1 m at the head to 30 m at the estuary, with all the components of soil including sand, silt, and clay, contributing to the formation of the streambeds of the island watersheds, making them weakly permeable through reduced hydraulic conductivity [54].

Several numerical and conceptual methods have been reported in the literature for GWL estimation. For example, Mohammadi [58] tested artificial neural network (ANN) models and MODFLOW to simulate the monthly GWLs of Karstic aquifers in Iran. The results indicated that the ANN models require less input data and time to run as compared to conventional models, such as MODFLOW. Several experiments in GWL modeling have shown that ANNs could be the better alternative over conceptual models [59]. Mohanty et al. [60] found that ANNs are better predictors of GWLs than MODFLOW for short term predictions. Karandish and Šimůnek [61] compared artificial intelligence (AI) methods with physical modeling. Results indicated that the AI methods performed well in water-

stressed conditions as compared to HYDRUS-2D. Therefore, AI methods provide promising tools for GWL predictions [30]. Several AI methods have been used by many researchers because of their simplicity and acceptable performance in different parts of the world [59].

Deep learning has been used to solve real-world problems relating to multi-magnitude data [62], determining the bearing capacity of concrete-steel columns [63], soil liquefaction [64], and solving genetic algorithms [65]. Deep learning and ANNs handle the non-linear behavior of time series better than regular regression [59]. Several hydrological parameters such as precipitation, streamflow, and GWLs exhibit time dependence and can be treated as time series functions. Time series functions usually exhibit non-linear relations, which are difficult to handle with simple static models. A multilayer perceptron (MLP), being the simplest kind of ANN, can approximate the functions related to dynamic hydrological problems that are difficult to model with numerical static methods. Similarly, an MLP can also predict values from a correlated input variable, which may be mapped with an output variable. For example, Sahoo and Jha [66] compared multiple regression and ANNs with a Levenberg Marquardt (LM) algorithm to predict GWLs in Kochi Prefecture of Shikoku Island, Japan. Graphical findings and analysis suggested the superiority of ANNs over multiple regression. Kouziokas et al. [67] used an MLP neural network with four different algorithms to forecast daily GWLs in Pennsylvania, USA. Temperature, humidity, and precipitation were used as input variables to predict GWLs. The four algorithms used in the study were Resilient Backpropagation (RB), LM, the Scaled Conjugate Gradient, and the BFGS Quasi-Newton. The LM algorithm performed better than the other algorithms in the prediction of GWLs. Juan et al. [68] developed two MLPs with an LM algorithm and

two sets of input data, i.e., temperature–precipitation–GWL and temperature–precipitation in Qinghai-Tibet plateau, China. The MLP models with 3-input variables performed better than the 2-input variables.

Because of the relatively simple structure of the MLP, it is not possible for these models to store the previous information in the time series, unlike an RNN. An RNN contains a memory block for storing previous steps of information in time series problems. Coulibaly et al. [69] compared three types of ANN models using GWL, precipitation, and temperature time series as input variables to simulate monthly GWLs in the Gondo aquifer, Burkina Faso. The results were also compared with radial basis function networks, generalized radial basis functions, and probabilistic neural networks. The results suggested that the RNN is the most efficient model compared to static structure ANNs. Furthermore, generalized radial basis functions are poorly performing models in monthly GWL simulations when compared to others. Müller et al. [70] compared an MLP with an RNN and more advanced ANNs to predict GWLs in Butte County, California, USA. They used three different methods to optimize model hyperparameters including two surrogate model-based algorithms and one random sampling method. They used stream flow, precipitation, and ambient temperature as input variables and estimated the GWLs after training these models. The results suggested that the MLP performed better than the ANNs, including LSTM and the convolutional neural network (CNN). Babu et al. [71] compared different algorithms to evaluate the RNN in GWL forecasting in Karnataka, India. They compared the LM, gradient descent with momentum, and the adaptive learning rate back propagation algorithm in predicting GWLs with the RNN. Their results suggested that the LM algorithm performed better with the RNN than all other algorithms in GWL modeling.

Although RNNs are enabled to store the previous information in their memory blocks, in large time series sequences the vanishing gradient problem hampers the learning of these models. The vanishing gradient problem in the RNN occurs when gradient updates become very small and add no significant difference to overall learning. To overcome the vanishing gradient problems of RNNs, more advanced models such as LSTM were introduced, and these are capable of storing important information with long sequences. Recently, Zhang et al. [30] conducted a similar study in which they compared LSTM with an MLP to predict GWLs in the Hetao irrigation district, China. Monthly water diversion, evaporation, precipitation, temperature, and time were used as input data to predict water table depth. Their results suggested that the LSTM model performed better than the MLP and could contribute to a strong learning ability on time series data. However, they did not include a detailed comparison of several input combinations for developing less data-intense models. Similarly, the more advanced time series models such as the CNN were not included.

The CNNs are the more advanced ANNs with usually a high number of hidden layers as compared to the RNN and the MLP. CNNs have gained popularity in terms of image data; however, they can perform equally well on time series data if modeled accordingly. Because of the more advanced functions of CNNs, such as convolution and max-pooling, these models have proved to be very promising in time series prediction. However, there is very limited literature available on GWL modeling using CNNs. Lähivaara et al. [72] used CNNs to estimate the GWLs and groundwater storage using seismic data. They applied the Galerkin method to model wave propagation followed by deep CNNs for parameter estimations and found that CNNs can extract additional information from seismic data about the aquifer.

The review literature suggests that the MLP and LSTM are promising methods that have been successfully used in many time series problems related to GWL modeling. In addition to the MLP and LSTM, the CNN, a relatively new method, was used in this study to investigate GWL estimation in the Long Creek and Baltic River watersheds of Prince Edward Island. The reason behind conducting this research was that it is currently not feasible for groundwater managers to manage the large number of watersheds in Prince Edward Island due to the small number of monitoring wells. The challenges of this study involve the unavailability of guidelines for selecting appropriate input variables for the optimum prediction of GWLs. Therefore, most of the input variables have been selected based on data availability. The specific objective of this study was to select appropriate ANNs and the best combination of input variables for the accurate possible estimation of GWLs.

4.2 Materials and Methods

4.2.1 Site Selection

Prince Edward Island is the smallest but most populous Atlantic Canadian province, having a pastoral landscape consisting of several rolling hills, woods, reddish white sand beaches, ocean coves, and red soil. With the uneven topography of Prince Edward Island, its streams are mostly non-contagious. For this study, the Baltic River and Long Creek watersheds situated in the center of Prince Edward Island were selected as experimental watersheds because of the relatively large number of irrigation wells in the area that might have contributing fluctuations in GWLs (Figure 4-1).

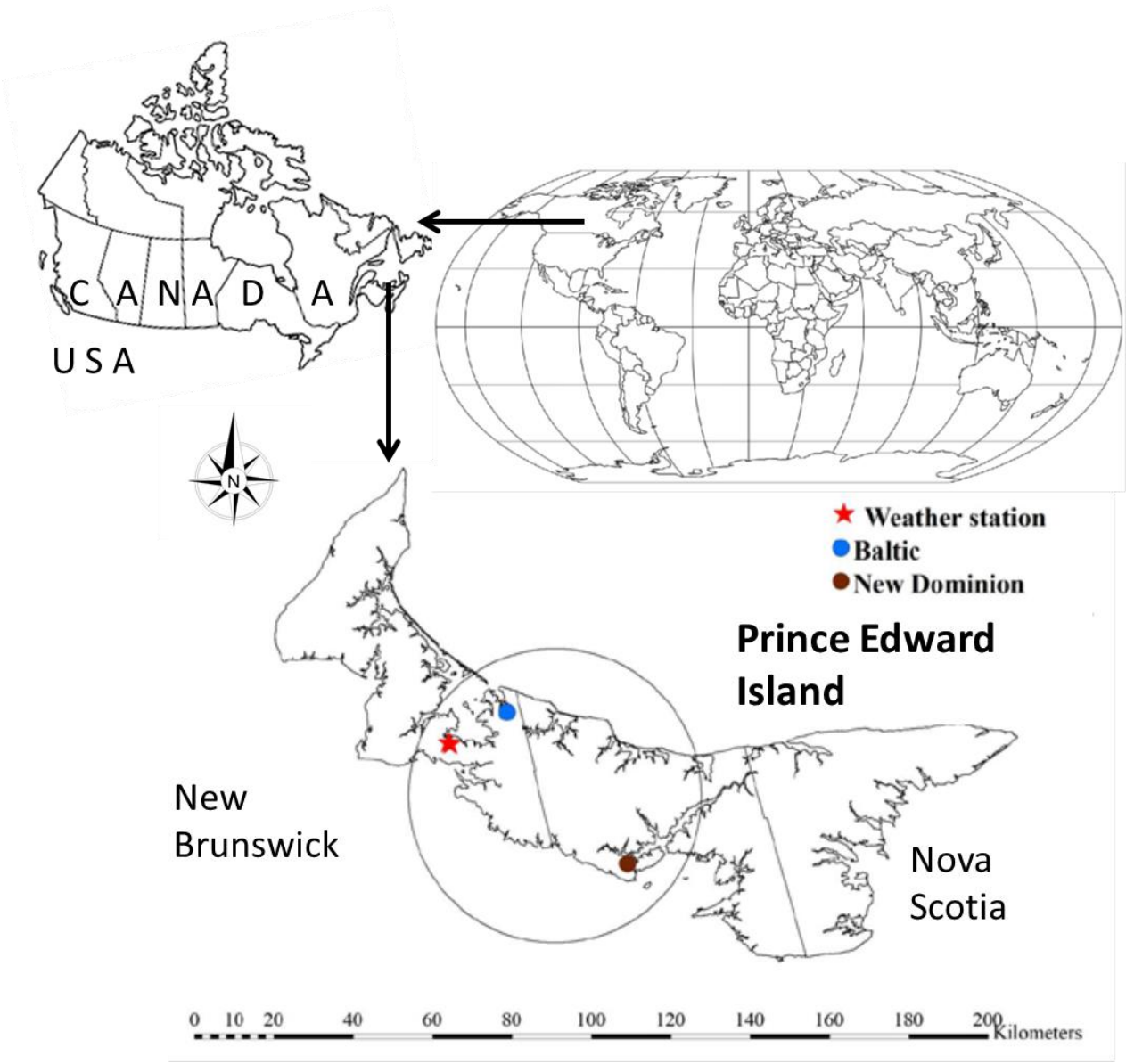

Figure 4-1 Locations of the experimental watersheds and the weather station in Prince Edward Island, Canada. The area of the relatively large number of irrigation wells has been encircled

4.2.2 Data Collection

Two monitoring wells, the Baltic (46.51000° N, 63.648056° W) and New Dominion (46.170278° N, 63.250000° W) wells, were selected for collection of actual GWL data of the Baltic River and Long Creek watersheds, respectively. The Baltic groundwater monitoring well was installed in the Baltic River watershed at an elevation of 25 m above

mean sea level. The New Dominion groundwater monitoring well was installed in the Long Creek watershed at an elevation of 19.93 m above mean sea level. Daily groundwater level data of these two monitoring wells for a seven-year period (2011–2017) was obtained from the Department of Communities, Land and Environment, Prince Edward Island. Weather data for this period was collected from a local weather station in Summerside (46.3934° N, 63.7902° W). The data included mean temperature, dewpoint temperature, heat degree days, precipitation, relative humidity, ETo, stream level, and stream flow. These data were used as input variables for the modeling of GWLs. The ETo was calculated using the Penman Monteith FAO-56 method.

4.2.3 Regression Subset Analysis for Input Variable Selection

Regression subset analysis was conducted to choose the appropriate variables, several combinations of which were used to select input variables for the deep learning models. The basic subset regression analysis was conducted in Minitab software (Version 18). Best Subsets Regression compares the different regression models that contain subsets of the specified predictors. The best-fitting models are suggested by Minitab containing one predictor, two predictors, and so on. Based on the highest regression, four input variable combinations were tested, namely 1-input variable, 2-input variable, 3-input variable, and 4-input variable combinations.

4.2.4 The Multilayer Perceptron for Groundwater Level Modeling

The multilayer perception is the simplest type of ANNs, which are biologically inspired computation models comprised of several layers, namely input, hidden, and output layers. All layers are connected each other with neurons—a basic processing unit of ANNs.

Input layers take all the input variables such as temperature, precipitation, etc. to predict output variables such as GWLs. Hidden and output layers handle the weights and biases from input layers through activation functions. The most common activation functions are the rectified linear unit (relu), sigmoid, and tanh. In modeling, sigmoid activation function is the most common function [73]. However, for this study, the rectified linear unit was selected for its better performance than the others. Most of the reviewed papers used trial and error methods to model the ANN layers and neurons [59]. For this study, two hidden layers and 100 neurons performed better. The MLP requires training data to adjust weight and bias for optimal prediction. Several learning algorithms have been used by modelers, such as back propagation, the LM, Bayesian regularization, adaptive learning rate back propagation, and gradient descent with momentum. Krishna et al. [74] compared several training algorithms in the groundwater modeling of an urban coastal aquifer in Andhra Pradesh state, India. They found that the LM algorithm was among the best learning algorithms compared to others. It is the most common algorithm in groundwater modeling. This algorithm works better for determining the local minima of error functions, resulting in increased prediction accuracy. For this study, the LM algorithm was selected to determine loss function. The MLP was used in this study for various input variable combinations (Figure 4-2).

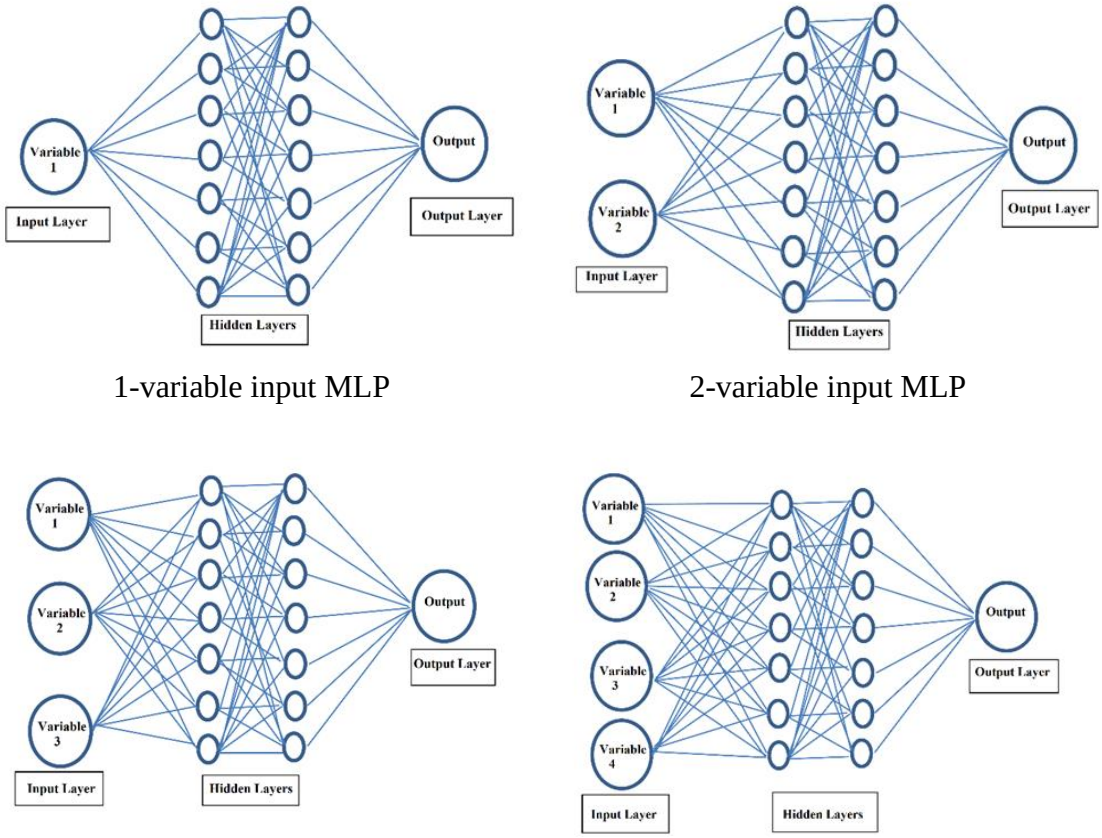

Figure 4-2 The multilayer perceptron (MLP) model for various input variable combinations

4.2.5 Long Short-Term Memory Neural Networks

The LSTM neural network is a special kind of RNN, which is a sequence-based model that can store and relate the previous information in a sequence, enabling it to predict time series problems. However, RNNs cannot store longer sequences because of the gradient vanishing problem in early layers. Gradient vanishing in an early layer is sometimes referred to as short-term memory neural networks. All RNNs form a chain-like structure as the information flows through them (Figure 4-3a). The RNNs store information in each stage based on time/sequence steps in the form of a hidden state, i.e., h_t for each input X_t. The tanh function in the memory block of an RNN scales the input data between −1 and 1.

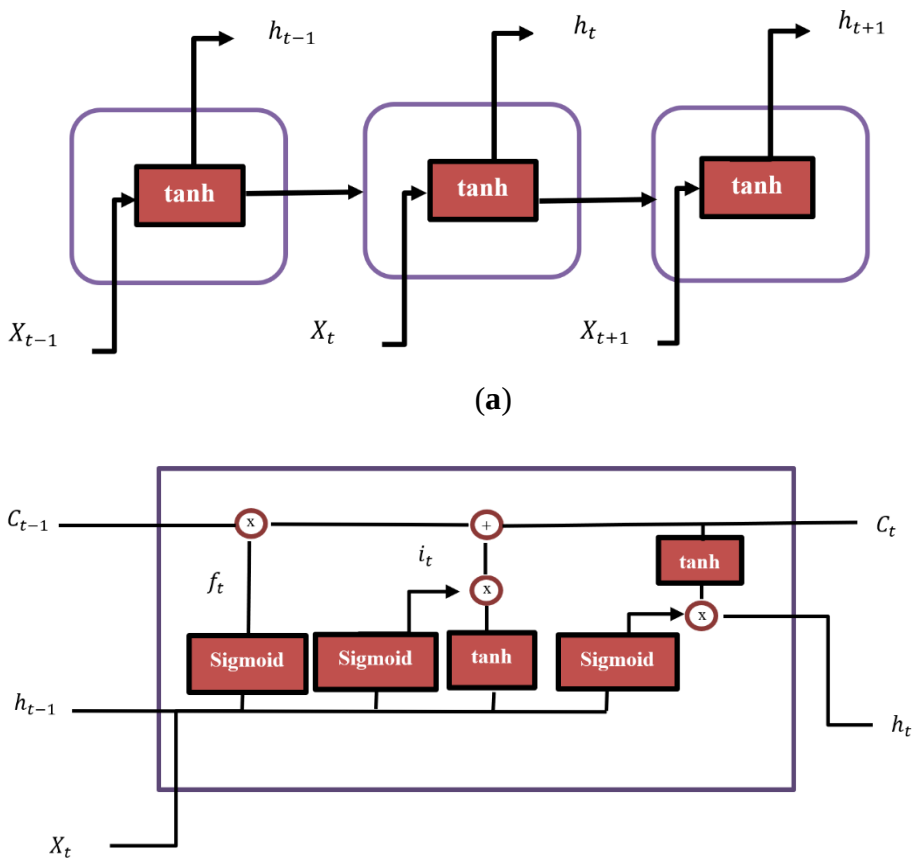

Figure 4-3 The memory block of (a) recurrent neural networks (RNNs) and (b) long short term memory (LSTM) neural networks

The LSTM addresses short-term memory problems by adding more states in the memory blocks of the RNN. In LSTM, a forget state (f_t) and a cell state (C_t) are added to retain the temporal and sequal dependence of previous blocks. The f_t in LSTM has the ability to discard or keep the information based on the sigmoid function output values. The values closer to 1 are kept, and those closer to 0 are forgotten. After passing f_t, the input variable X_t and the previous cell hidden state h_{t-1} are passed through the sigmoid and tanh functions. The dot product of the tanh and sigmoid functions are then added with f_t to

compute C_t. The more detailed overview of LSTM information flow memory block is described in Figure 4-3b.

4.2.6 Convolutional Neural Networks

CNNs are mostly used for machine vision applcations in two-dimensional (2D) images. However, a one-dimensional (1D) CNN has several applications in time series classification and natural language processing. Use of a 1D CNN in GWL modeling is very limited in the literature. Convolution layers convolute the feature on 1D matrices. Because of fewer dimensions, the convolution filters have less processing work, making them computationally faster than 2D CNN. There has been very limited research conducted on GWL modeling using CNNs. However, based on the hit and trial method, five layers were used in the CNN in this study. The first layer was the convolulational layer followed by a maxpooling layer to extract features. To connect the maxpooling layer with the fully connected layers, a third, flatten layer was added. The last two layers were fully connected or dense layers to obtain the output vectors (Figure 4-4).

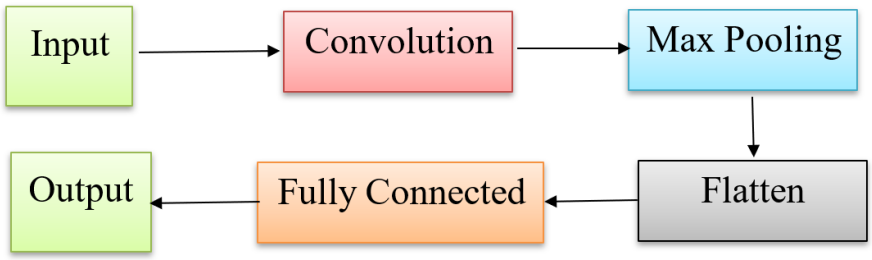

Figure 4- 4 Architecture of the 1D CNN

4.2.7 Hyperparameter Tuning of ANNs

The tuned parameters were selected for different ANNs based on the highest accuracy using the hit and trial method. All ANNs were trained from scratch using hyperparameters including activation functions, number of neurons, number of layers, neurons, optimization, and learning rate. For the MLP, these respective hyperparameters were Relu, 2, 100, Adam, and 10^{-3}. For LSTM and the CNN, the activation functions were Tanh and Relu, and the neurons were 50 and 64, respectively. The CNN had 5 layers. The rest of the hyperparameters for LSTM and the CNN were the same as those of the MLP.

4.2.8 Model Evaluation Criteria

The model performance was evaluated by loss functions. The root means square error (RMSE) is well known model evaluation criteria used in various studies to evaluate the model performance [75][76]. It squares the difference between predicted and actual value and may range between 0 and1.

GWLs were plotted against actual GWLs and against a 1:1 line to evaluate the over- or under-estimation of GWLs overlapping and its scattering/clustering. To overcome the noisy effects of the large data points used in this study, a data normalization technique was performed. The max-min normalization performed well with this set of data. However, after the model training, the data were back transformed to show trends in the figures.

4.3 Results and Discussion

4.3.1 Descriptive Statistics of Input Variables

The descriptive statistics of several input variables for GWL modeling are displayed in Table 4-1. The mean temperature ranged between −22.5 and 26.5 °C in Summerside,

Prince Edward Island, in the 2011–2017 period. The difference between mean temperature and median temperature is −0.291 °C, which depicts a slightly skewed distribution of mean temperature. The dewpoint temperature ranged between −27.692 and 21.775 °C. The dewpoint temperature distribution showed slightly more skewness than the mean temperature. Because of seasonality, both the mean temperature and the dewpoint temperature show a bimodal distribution. The relative humidity of selected region ranges between 46.7 to 98.25% for year 2011–2017. Because of the high variation, the relative humidity showed a high standard deviation for such a large dataset. The heating degree days ranged between 0 and 40.5°C from 2011 to 2017. Because of a high frequency of 0 °C values of heat degree days in winter, the distribution has a high peak and skews towards the right. The ETo ranges between 0.0839 and 7.2631 mm/day. Because of the high number of cold days in Prince Edward Island, the distribution of ETo is right-skewed with a skewness of 0.74. However, because of a lower variability in the ETo range, it has a lower standard deviation. The island received a total precipitation of 753 to 1070.3 mm/year for the years from 2011 to 2017. The daily precipitation received by the island is highly variable, i.e., 0–103.8 mm/day. Because of storms and a lack of rainfall on several days of any given year, the precipitation distribution is highly right-skewed with a skewness coefficient of 5.72. Daily water level fluctuations in the Baltic groundwater monitoring well located in the Baltic River watershed range between 13.1 and 18.6 m in the years 2011–2017. Because of lower fluctuations in GWLs, the standard deviation is lower, i.e., 0.93 m. The distribution of the Baltic River GWLs showed right skewness, with a skewness coefficient of 0.58. Daily water level fluctuations in the New Dominion groundwater monitoring well, located in the Long Creek watershed, range between 9.16 and 18.12 m in

the years between 2011 and 2017. Because of the high fluctuations in the Long Creek GWLs compared with the Baltic River GWLs, the standard deviation is relatively high, i.e., 1.58 m. The Long Creek distribution showed a right skewness, with a skewness coefficient of 0.58. The associated stream discharge for the Long Creek and Baltic River monitoring wells is 0.46–42.4 m^3/s and 0.548–51 m^3/s, respectively.

Table 4-1 Descriptive statistics of input and output variables for groundwater level modeling.

Variable	Maximum	Minimum	Mean ± SD	Skewness
Mean temperature (°C)	26.5	−22.5	6.41 ± 10.4	−0.26
Dew point temperature (°C)	21.8	−28.0	2.66 ± 10.2	−0.33
Relative humidity (%)	98.3	46.7	77.7 ± 10.2	−0.37
Heat degree days (°C)	40.5	0.00	12.0 ± 9.90	0.40
Reference evapotranspiration (mm/day)	7.26	0.08	2.05 ± 1.50	0.74
Precipitation (mm)	103.8	0.00	2.41 ± 6.14	5.72
The Baltic River watershed daily groundwater levels (m)	18.6	13.1	14.6 ± 0.93	0.58
Stream flow for the Baltic River watershed (m^3/s)	51.0	0.548	2.65 ± 3.21	7.57
Stream level for the Baltic River watershed (m)	2.14	0.50	0.68 ± 0.15	2.99
The Long Creek watershed daily groundwater levels (m)	18.1	9.16	12.8 ± 1.58	0.06
Stream flow for the Long Creek watershed (m^3/s)	42.4	0.46	2.00 ± 2.21	7.04
Stream level for the Long Creek watershed (m)	2.84	1.06	1.25 ± 0.17	2.51

The distribution of the stream discharge for both monitoring wells showed a right skewness, with a skewness coefficient greater than 7. A high skewness coefficient reflects the high occurrence of peak flow levels probably during storms. The associated stream levels for the New Dominion and Baltic monitoring wells are 1.055–2.835 m and 0.5–2.14 m, respectively. Similar trends can be seen with the stream levels associated with both monitoring wells, i.e., a high skewness coefficient.

4.3.2 Regression Subset Analysis for Variable Selection

For the 1-input variable combination, stream level was found to be the highest contributor among the eight selected different variables for the Baltic and New Dominion monitoring wells. The correlation coefficient for the Baltic River GWLs and the associated stream level was found to be 0.508. Similarly, the correlation coefficient between the Long Creek GWLs and the associated stream level was found to be 0.49. For the 2-input variables combinations, stream flow and stream levels were selected for the Baltic River watershed with a coefficient correlation of 0.63. For the Long Creek watershed, stream level and dew point temperature proved to be the best input variables for the 2-input variable combinations. For the 3-input variable combinations, stream level, stream flow, and evapotranspiration were selected for the Baltic River watershed, with a slightly high correlation coefficient of 0.658 compared with that of the 2-input variable combinations. Stream level mean temperature and evapotranspiration variables were selected for the Long Creek watershed, with a low coefficient correlation of 0.572 compared with that of the Baltic River watershed 3-input variable combinations (Table 4-2). Four-input variables did not add much toward defining GWL variability, i.e., only 0.4 and 2.2% increases in correlation coefficients for the Baltic River and Long Creek watersheds, respectively. Interestingly, the precipitation variable did not contribute towards GWL fluctuations for both watersheds. A comparative study of GWL modeling using AI methods [59] reported that precipitation was used 48 times in GWL modeling. Statistical analysis, specifically in regression analysis, should be conducted to select appropriate input variables for groundwater modeling using AI methods [59]. Several studies have used past GWLs for

time series forecasting however, in this study, prediction models were used to predict GWLs from other input variables.

Table 4-2 Correlation analysis of input variable selection plotted/regressed versus actual GWLs.

Watershed	Number of Variables	Variables	R^2
Baltic River	1	Stream level	0.51
		Stream flow	0.2.8
	2	Stream level and stream flow	0.63
		Stream level and precipitation	0.51
	3	Stream level, stream flow and evapotranspiration	0.66
		Stream level, stream flow and Mean temperature	0.64
	4	Stream level, stream flow, heat degree days and evapotranspiration	0.66
		Stream level, stream flow, mean temperature and evapotranspiration	0.66
Long Creek	1	Stream level	0.49
		Stream flow	0.36
	2	Stream level and Dew point temperature	0.55
		Stream level and dew heat degree days	0.55
	3	Stream level, mean temperature and evapotranspiration	0.57
		Stream level, stream flow and heat degree days	0.57
	4	Stream level, dew point temperature, relative humidity, evapotranspiration	0.59
		Stream level, relative humidity, mean temperature and evapotranspiration	0.58

4.3.3 The 1-Input Variable Model

For the 1-input variable deep learning model, the last epoch training and validation losses of the MLP for the Baltic River watershed were recorded to be 0.0839 and 0.0818, respectively. A similar training loss of the MLP for the Long Creek watershed was recorded, i.e., 0.0856. However, the validation loss of the MLP for the Long Creek watershed was 25% higher than the Baltic River watershed (Table 4-3). The training and validation losses in the LSTM model for the Baltic River watershed were not substantially different from the MLP and were recorded to be, respectively, 0.0832 and 0.074. A trend of a higher validation loss in the LSTM model, similar to that of the MLP for the Long

Creek watershed, was observed, i.e., the validation loss was 23% higher than the training loss.

Table 4-3 Training and validation losses, and the root mean square error (RMSE) of the artificial neural networks (MLP, LSTM, and CNN) used in this study for the Baltic River and Long Creek watersheds using 1-, 2-, 3-, and 4-input variables

Watersheds	No. of Variables	Method	Training Loss	Validation Loss	Training RMSE	Validation RMSE	R^2
Baltic River	1	MLP	0.084	0.082	0.567	0.558	0.65
		LSTM	0.083	0.074	0.557	0.530	0.66
		CNN	0.010	0.010	0.556	0.550	0.66
Long Creek		MLP	0.086	0.110	0.957	1.169	0.63
		LSTM	0.085	0.110	0.973	1.173	0.62
		CNN	0.013	0.017	0.948	1.180	0.63
Baltic River	2	MLP	0.081	0.072	0.560	0.512	0.66
		LSTM	0.083	0.076	0.561	0.531	0.66
		CNN	0.011	0.010	0.549	0.549	0.66
Long Creek		MLP	0.081	0.107	0.929	1.180	0.64
		LSTM	0.083	0.108	0.940	1.210	0.64
		CNN	0.011	0.018	0.898	1.215	0.65
Baltic River	3	MLP	0.079	0.065	0.545	0.474	0.69
		LSTM	0.079	0.067	0.539	0.483	0.69
		CNN	0.010	0.009	0.503	0.529	0.71
Long Creek		MLP	0.082	0.107	0.945	1.160	0.64
		LSTM	0.083	0.110	0.943	1.203	0.63
		CNN	0.011	0.018	0.888	1.209	0.66
Baltic River	4	MLP	0.079	0.064	0.543	0.471	0.69
		LSTM	0.077	0.066	0.534	0.480	0.69
		CNN	0.010	0.009	0.505	0.532	0.71
Long Creek		MLP	0.078	0.103	0.912	1.150	0.66
		LSTM	0.080	0.106	0.916	1.200	0.67
		CNN	0.009	0.017	0.813	1.170	0.70

Both the MLP and LSTM models performed poorly in the validation stage for the Long Creek watershed. However, for both watersheds, the training and validation losses of the 1D CNN were lower than those of the LSTM and MLP models. For the Baltic River watershed, the training and validation loss of the CNN was 0.01. The training and validation losses of the CNN for the Long Creek watershed were recorded to be 0.0125

and 0.0174, respectively. Figure 4-5 shows the training and validation phases of the deep learning models for the Baltic River and Long Creek watersheds. For both watersheds, the deep learning models were unable to predict the lower peaks very well. Variation in estimations of peaks were found to be higher in the training phase compared with that in the validation phases of all ANNs.

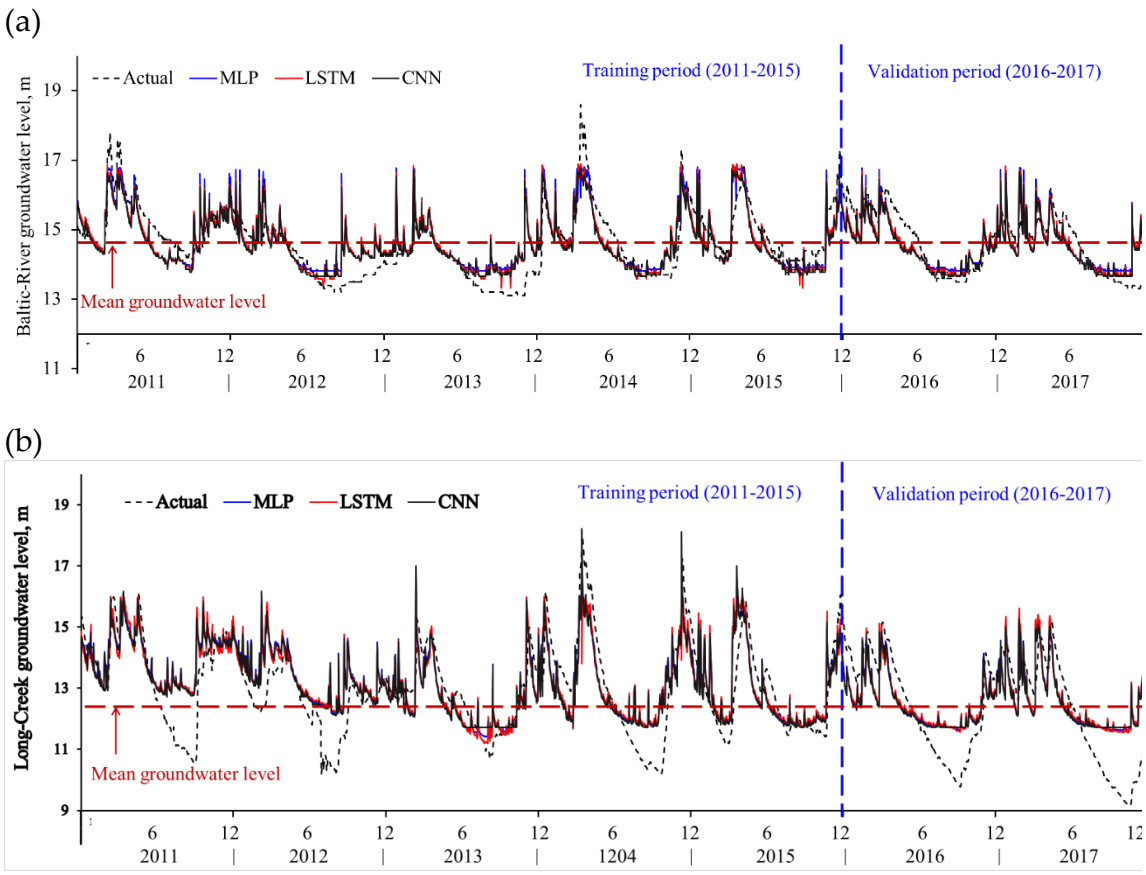

Figure 4-5 Training and validation phase of the 1-input variable models for (a) Baltic-River watershed and (b) Long-Creek watershed

4.3.4 The 2-Input Variable Models

The 2-input variable MLP model for the Baltic River watershed showed training and validation losses of 0.0814 and 0.0723, respectively. These losses were slightly lower than the losses of the 1-input variable MLP models. Similarly, the 2-input variable MLP models

training and validation losses for the Long Creek watershed were 0.0816 and 0.1068, respectively. The 2-input variable LSTM training losses for the Baltic River watershed improved by 0.8%, and the validation loss decreased by 0.2% in comparison with the 1-input variable models. In comparison with the training losses of the 1-input variable CNN, those of the 2-input variable CNN slightly increased from 0.0100 to 0.0113 and from 0.0100 to 0.0174, with no change in validation loss, for the Baltic River watershed. For the Long Creek watershed, the training loss was reduced from 0.0125 to 0.0112, and the validation loss increased from 0.0174 to 0.0184, in comparison with the 1-input variable CNN. The training and validation phases showed slight improvements in GWL estimation. However, no major difference was observed in GWL predictions in the 1-input and 2-inputs variable combinations, i.e., the lower peaks of the estimated GWLs did not match the lower peaks of the actual GWLs.

4.3.5 The 3-Input Variable Models

The 3-input variable MLP model for the Baltic River watershed showed slight improvements in training loss (0.079) and validation loss (0.0648) compared with the 2-input variable MLP model. However, the training loss of the 3-input variable MLP for the Long Creek watershed was lower, i.e., 0.0816, and the validation loss (0.1067) was slightly improved, compared with the 2-input variable MLP model. The 3-input variable LSTM model for the Baltic River watershed showed a higher validation loss (0.0673) as well as a training loss (0.079) that was similar to that of the 3-input variable MLP model. The 3-input variable LSTM model for the Long Creek watershed had a higher training loss (0.0832) and a higher validation loss (0.1095) compared with the 2-input variable LSTM

model for the same watershed. The 3-input CNN model for the Baltic River watershed showed the lowest training loss (0.0101) and validation loss (0.0093) compared with all 3-input variable models. Similarly, the 3-input variable CNN model for the Long Creek watershed showed the lowest training loss (0.011) and validation loss (0.0182) compared with all 3-input variable models. There was close agreement between the actual and estimated GWLs for the Baltic River watershed. However, there was weak agreement between the lower peaks of the actual and estimated GWLs of the Long Creek watershed.

4.3.6 The 4-Input Variable Models

The 4-input variable MLP model for the Baltic River watershed showed no difference in training loss (0.079) and validation loss (0.0644) compared with the 3-input variable MLP model. Similarly, no major difference was observed in training and validation losses for the Long Creek watershed compared with the 4-input MLP model; they were found to be 0.0783 and 0.1031, respectively. For the 4-input variable LSTM model, the training and validation losses for the Baltic River watershed were recorded as 0.077 and 0.0663, respectively. The 4-input variable LSTM model for the Long Creek watershed showed a slight improvement in training (0.0798) and validation (0.1057) losses compared with the other LSTM models. The 4-input variable CNN models showed the lowest training and validation losses for both the Baltic River and Long Creek watersheds compared with all other 4-input variable models. The addition of a fourth variable reduced the difference between the lower peaks of the estimated and actual GWLs as observed in the case of the 1-input and 2-input combinations (Figure 4-6). A close agreement between the actual and the estimated GWLs for the Baltic River watershed was observed, as in the output of the

3-input variable model, and a comparatively weak agreement was observed between the lower peaks of the actual and the estimated GWLs of the Long Creek watershed.

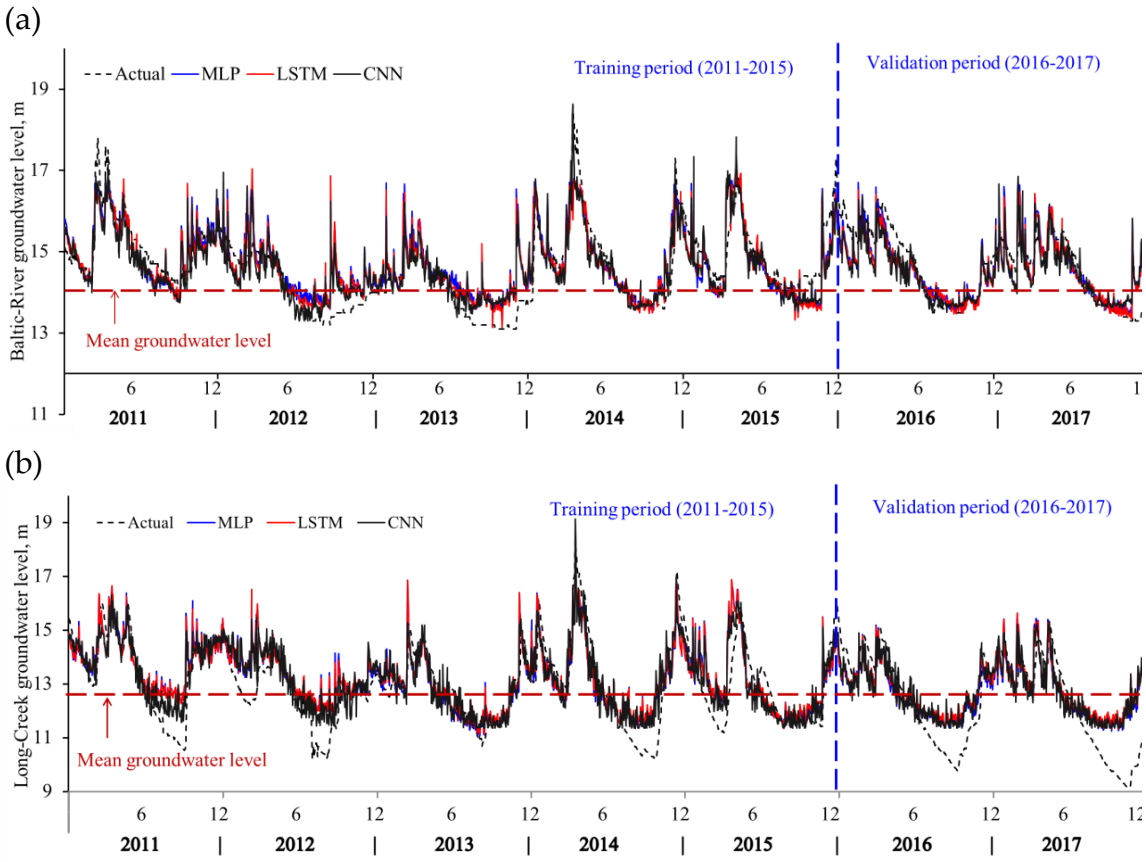

Figure 4-6 Training and validation phases of the 4-input variable models for (a) Baltic-River watershed and (b) Long-Creek watershed

4.3.7 Model Evaluation

The RMSE of the 1-input variable model for the Baltic River watershed was lower than the Long Creek watershed for all ANN models (Table 4-3). For the 1-input variable Baltic River watershed LSTM, the RMSE (0.53 m) was lower at the validation stage than both the MLP and the CNN. However, in the training stage of the 1-input variable model

for the Baltic River watershed, the CNN performed better than the other models, with an RMSE of 0.556 m. For the 1-input variable models of the Long Creek watershed, higher validation losses, as compared to training losses, were recorded. The 1-input variable model of the MLP performed well in the validation stage, with a recorded RMSE of 1.169 m for the Long Creek watershed. At the training stage for the Long Creek watershed, the 1-input variable CNN performed well, with a slightly lower RMSE, i.e., 0.948 m. Similar trends were recorded for the 2-input variable ANNs, with a slight improvement in the recorded RMSE for both training and validation stages. For the Baltic River watershed, the 2-input variable MLP model performed well at the validation stage, with a slightly lower RMSE, i.e., 0.56 m. However, it was not much different than the 1-input variable model, as the RMSE was improved only by 0.046 m. Similarly, the CNN improved the training stage error of the 2-input variable models by 0.007 m. The slightly reduced RMSE indicates the better performance of the 2-input variable MLP and CNN models in comparison with the 1-input variable models for the Baltic River watershed. For the Long Creek validation stage, the 2-input variable models performed poorly compared with the 1-input variable models. The 2-input variable MLP performed better than the LSTM and CNN models, with a recorded RMSE of 1.18, which was higher in comparison with the 1-input variable MLP model. The 2-input variable CNN model performed better at the training stage for the Long Creek watershed, with a slight improvement in RMSE (0.898) compared with the 1-input variable CNN model. The 3-input variable MLP model for the Baltic River watershed performed well, reducing the RMSE by 0.038 m in comparison with the 2-input variable MLP model. The CNN performed well at the training stage for the Baltic River watershed, with an improved RMSE of 0.066 m. For the Long Creek watershed, the 3-input variable

MLP model performed well, with an improved RMSE of 0.02 m, as did the CNN, with an RMSE of 0.01 m in the validation and training stages, respectively. The smaller differences in RMSE indicate the slightly improved performance of the 3-input variable models over the 2-input variable models for the same site. The 4-input variable MLP model for the Baltic River watershed performed well at the validation stage, with an RMSE of 0.471, compared with all the models used in this study. Similarly, the 4-input variable MLP model for the Long Creek watershed achieved the lowest RMSE (1.15) in the validation stage. The reduction of the RMSE, achieved by increasing the number of variables, suggests that the selected variables slightly increased the performance and overall efficiency of the ANNs. In general, no major effect on model performance was observed by increasing the number of variables. The major contributor in defining the GWL variation was the stream level. The reason for this could be the inability of the remaining three variables to account for the variability in GWLs. Evidence of this trend is presented in Table 2. The increase in the number of variables does not show any major effects on the coefficient of determination.

The potential reason for the low performance of ANNs on the Long Creek watershed could be the absence of a lurking input variable, such as pumping data. There is no data available on actual daily pumping usage by high-capacity well owners. Most of the lower peaks were recorded mostly in the summer season for the Long Creek watershed, as depicted in Figures 5 and 6; wells might be pumped by well owners in drought season for supplemental irrigation to replenish crop water requirements. However, pumping problems or lower peaks were not a major problem for the Baltic-River watershed, whereas high-capacity wells in that area was.

It is noticeable that the MLP, being the simplest type of ANN, performed well at the validation stages of both watersheds compared with the more advanced ANNs, including the LSTM and CNN models. In a similar study of GWL estimation using ANNs, Mueller et al. [70] reported that the MLP outperformed both the LSTM and CNN models. At the training stage, the performance of the CNN was greater than that of the other ANNs. This could be due to the additional parameter-learning functionalities in the CNN, such as the convolutional and max-pooling filters, which were not the part of the MLP and LSTM models.

Furthermore, polynomial relationships between the predicted and actual groundwater level suggest that increasing the number of variables from 1 to 4 increased the R^2 from 0.62 to 0.70 for the Long Creek watershed (Figure 4-7). A similar trend was observed for the Baltic River watershed as the R^2 was raised from 0.66 to 0.71 for the 1-input and 4-input variable models, respectively (Figure 4-8). These results suggest that the stream level and stream flow variables should be considered in defining the overall variability of GWLs. These variables contribute to the role of stream level and stream flow in a watershed, as reported in the literature [77]. Recent study conducted by Lee et al. [78] found the similar relationship between GWLs and stream level. Zhang et al. [30] compared feedforward neural networks with LSTM in GWL prediction in the Hetao irrigation district, China. Contrary to our findings, their results suggest that the LSTM model is a better predictor of GWL modeling than the MLP.

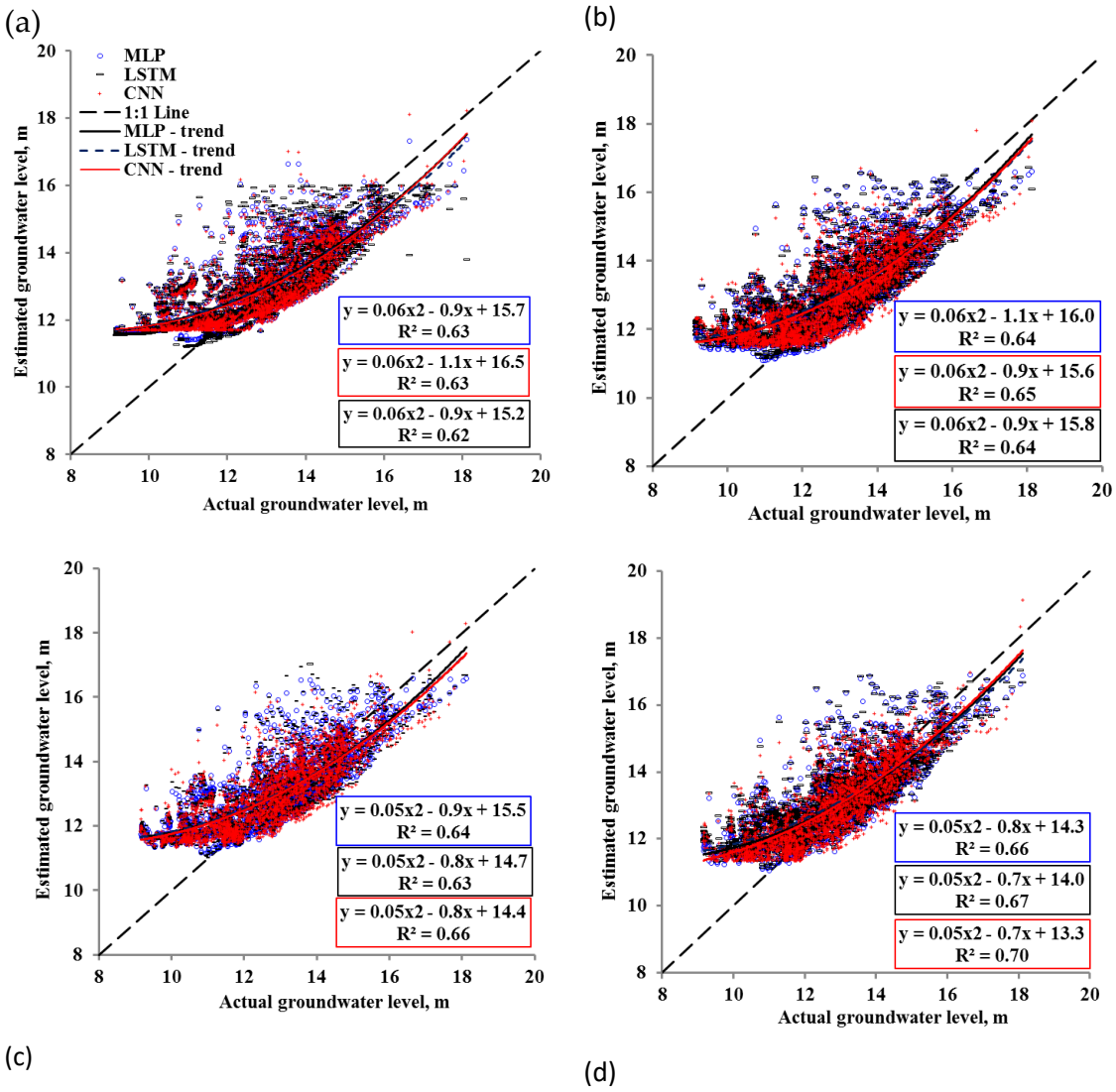

Figure 4-7 The Long Creek watershed estimated groundwater levels for (a) 1-input, (b) 2-input, (c) 3-input, and (d) 4-input variable models versus actual groundwater levels

The CNN performed better with a higher number of input variables compared with the LSTM and MLP models. For example, for both watersheds, the MLP performed slightly better than the CNN for the 1- and 2-input variable models. However, the accuracy of the CNN was higher than that of the MLP in the 3-and 4-input variable models for both watersheds (Figures 4-7 and 4-8).

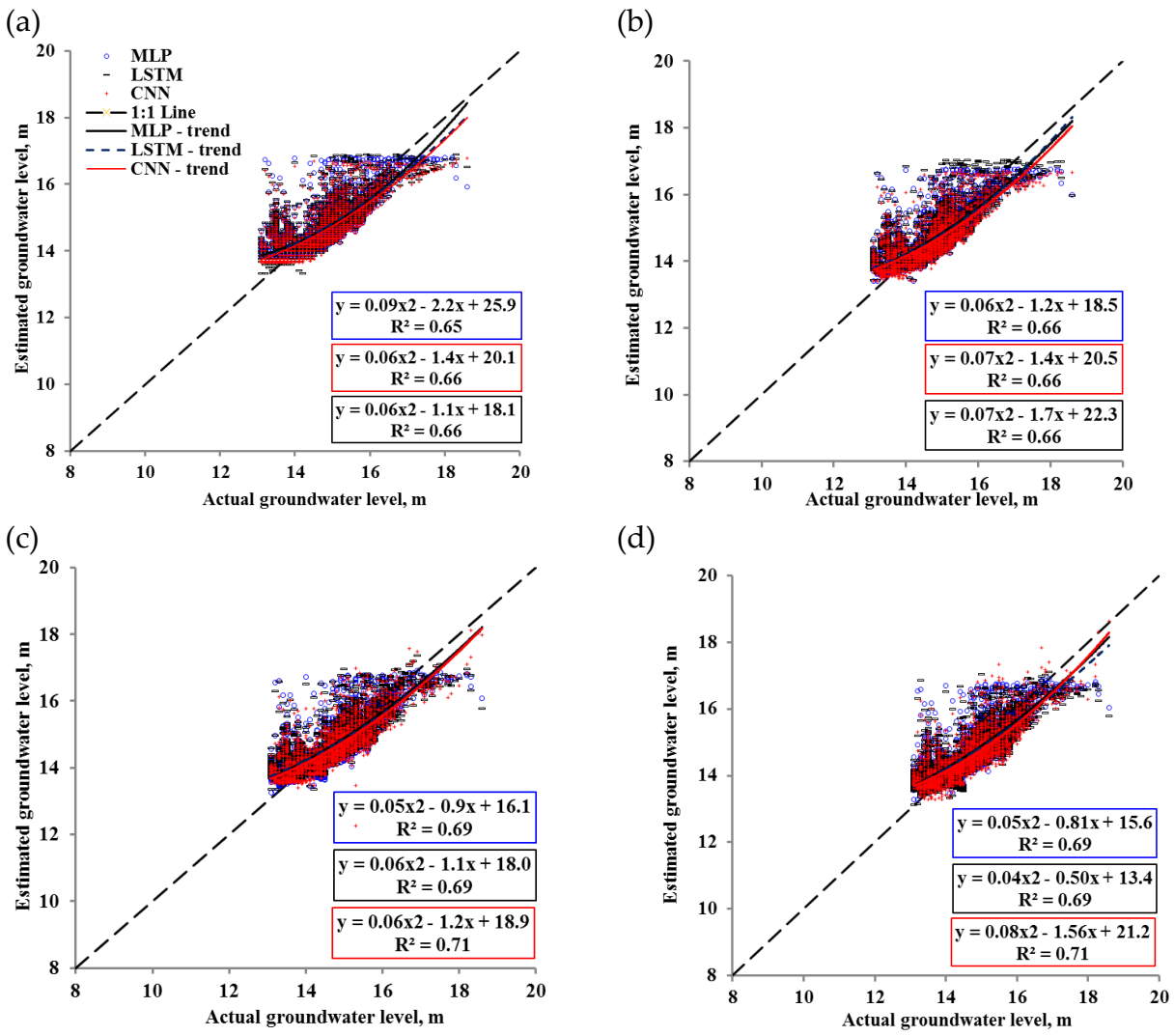

Figure 4-8 The Baltic River estimated groundwater levels for (a) 1-input, (b) 2-input, (c) 3-input, and (d) 4-input variable models versus actual groundwater levels

The higher accuracy of the CNN with a certain number of variables may indicate the advantage of the CNN in dealing with more complex relationships in comparison with the MLP and LSTM models. The additional functionalities of convolutions and max pooling helped the CNN to obtain higher accuracies with a higher number of inputs. However, the over-estimation of GWLs can be visualized for the Long Creek watershed for approximately below 11 m, and under-estimation can be visualized beyond the 13 m level. For the Baltic River watershed, the over- and under-estimations were approximately below

14 and beyond 15 m, respectively. The possible reason for the poorly matching peaks of the extreme GWLs may be due to short-time variations in the GWLs because of the pumping during water-deficient months and the quick recharge of groundwater from the higher level of groundwater neighboring the monitoring well. This means that there is a need to further investigate how the extreme GWLs can be estimated, especially for the lower peaks. Mismatch between the predicted and actual levels of groundwater could be due to several hydrogeological reasons, including the fact that groundwater pumping can also draw streamflow into connected aquifers, where pumping rates are relatively large or where the locations of pumping stations are relatively close to a stream [4]. The ANN models used in this study were unable to predict the lower groundwater peaks. This drawback can be addressed by adding more variables, such as actual pumping withdrawal, to develop more accurate models. In general, ANNs can predict human interventions if modeled with proper inputs. However, in this study, the groundwater pumping data were not available. Emphasis on the collection and storing of the pumping data is therefore recommended so that provincial water management authorities can track this important variable for groundwater sustainability on the island.

The application of these models can be further extended to other watersheds to estimate GWLs, as there are more than 250 watersheds in Prince Edward Island. The installation and maintenance of a large number of monitoring wells is neither feasible nor economical. These modeling techniques provide economical and convenient methods of equitable water distribution for water resource managers and policymakers in large areas.

4.4 Conclusions

In this study, deep learning has been used to test different ANN models with several input combinations to predict GWLs in the Baltic River and Long Creek watersheds in Prince Edward Island. The results suggest that ANNs can be used to predict GWLs in Prince Edward Island. The stream level was the most highly correlated factor in defining GWL fluctuations for both watersheds. All ANN models performed well on the Baltic River watershed in comparison with the Long Creek watershed. The number of variables had no major effect on the RMSE of either watershed. The results suggest that the GWLs of the Baltic River and Long Creek watersheds can be efficiently modeled with the stream level variable in the absence of GWL data. Similarly, for the Long Creek watershed, the GWLs can be modeled with stream levels with a slightly high RMSE as compared to the Baltic River watershed. The performance of the MLP at the validation stage was slightly greater than that of the MLP and LSTM models. However, at training stages, the CNN performed very well, with the lowest RMSE for both watersheds. The ANN models were unable to predict the lower peaks in the summer season, specifically for the Long Creek watershed, which could be due to lurking variables such as the pumping from high-capacity irrigation wells. It is also notable that the increased number of variables from 1 to 4 improved the RMSE for the Baltic River watershed by 11% only and for the Long Creek watershed by 1.6% only. It may be concluded that the GWLs in the Baltic River and Long Creek watersheds can be modeled using stream levels with RMSEs of only 0.53 and 1.169 m, respectively. The results also suggest that the CNN performed better with a higher number of input variables; however, the performance of the MLP was better with lower input variable models.

CHAPTER 5
Summary and Conclusions

With the background of variations in rainfall patters and importance of potato crop for the economy of Atlantic Canada, the research presented in this thesis was based on the hypothesis that the rainfall in Prince Edward Island is not enough for sustainable potato production in the island. The specific objectives of this study were to i) model evapotranspiration with artificial intelligence for precision water resource management, ii) determine the effects of different irrigation systems (sprinkler, drip, fertigation and control; rainfed) on potato tuber yield, quality, payout returns, and iii) model the groundwater levels of Prince Edward Island using deep learning methods to ensure sustainability of water balance in Prince Edward Island.

With the use of deep learning, ANNs and RNNs) namely MLP, and LSTMs the gaps between rainfall and ETo and fluctuations in GWLs were modelled. Irrigation methods namely drip, sprinkler and fertigation were tested in consideration with potato tuber yield, quality and payout returns. Reference and crop-specific evapotranspiration were precisely modelled for Prince Edward Island. No major differences were observed in the accuracy of different RNNs used in study; e.g., LSTM and bidirectional LSTM. The data from 2011-2017 showed that the months of June, July and August received lesser rainfall than ETc and other months to replenish the crop water requirements. Due to smaller kc factor of potato crop in earlier months, lesser amounts of irrigations may be required for replenishing potato water requirements. However, during tuber development/bulking stage, the shortage

of water may hinder the potential potato yield. The study results also showed the high variability in the monthly recorded rainfall, posing several challenges to water managers for sustainable water management. In order to maximize potato tuber yield, timely SI in addition to rainfall is one of the viable options.

Because of rainfed agriculture in Prince Edward Island, there are no guidelines available for selection of an appropriate irrigation method to achieve maximum water productivity. This study investigated several irrigation methods (sprinkler, drip, control and fertigation) in consideration with potato tuber yield, potato tuber quality, farm payout returns and water productivity. There were significant effects of SI methods on potato tuber yield, quality, payout returns and water productivity. Sprinkler and fertigation system performed comparatively better in 2018 and 2019 respectively in terms of potato tuber yield. Sprinkler irrigation system performed significantly better than other treatments in term of farm payout returns and potato tuber quality. However, the lowest water productivity was observed for sprinkler irrigation system due to higher water consumption by this method. In terms of water sustainability, fertigation was the most effective irrigation method in comparison with control and sprinkler irrigation application methods.

Commonly, irrigation especially sourced from groundwater pumping causes several environmental problems such as declined groundwater levels and saltwater intrusion. Therefore, the effects of groundwater pumping on groundwater levels were assessed for sustainable water management strategies. Since the physical measurement of groundwater levels is challenging with respect to the maintenance of groundwater wells and the collection of periodic dips, the techniques introduced in this study; i.e., the use of ANNs and RNNs, are convenient and accurate. Stream flow gauges are easier to manage than

physical measurement of fluctuations in groundwater levels. In areas where groundwater pumping is common for SI or for domestic use, the inventory control of groundwater resources could become more convenient with the technique used in this study. The analysis of two watersheds namely Baltic and Long creep showed that the deep learning methods used in this study were accurate to simulate fluctuations in groundwater levels. Because of the non-availability of daily pumping data in the island, it is recommended that provincial water resource management authorities should monitor groundwater pumping data on a regular basis.

References

1. MacDonald, M. Potatoes: A billion dollar industry for P.E.I. Available online: https://www.theguardian.pe.ca/news/local/potatoes-a-billion-dollar-industry-for-pei-95098/ (accessed on Jan 15, 2020).
2. Agriculture and Agri-Food Canada (AAFC) Potato Market Information Review 2016-2017. Available online: https://www5.agr.gc.ca/eng/industry-markets-and-trade/canadian-agri-food-sector-intelligence/horticulture/horticulture-sector-reports/potato-market-information-review-2016-2017/?id=1536104016530#a1.2.3 (accessed on Jan 15, 2020).
3. Steduto, P.; Hsiao, T.C.; Fereres, E.; Raes, D. *Crop yield response to water*; 2012;
4. Van Loon, C.D. The effect of water stress on potato growth, development, and yield. *Am. Potato J.* **1981**, *58*, 51–69.
5. Shock, C.C.; Pereira, A.B.; Eldredge, E.P. Irrigation best management practices for potato. In Proceedings of the American Journal of Potato Research; Potato Association of America, 2007; Vol. 84, pp. 29–37.
6. Shock, C.C.; Feibert, E.B.G.; Saunders, L.D. Potato yield and quality response to deficit irrigation. *HortScience* **1998**, *33*, 655–659.
7. Richards, W.; Daigle, R. *Scenarios and Guidance for Adaptation to Climate Change and Sea-Level Rise – NS and PEI Municipalities*; Atlantic Climate Adaptation Solutions Association, 2011;
8. Department of Communities, L. and E. Watershed Management on PEI | Prince Edward Island Available online: https://www.princeedwardisland.ca/en/information/communities-land-and-

environment/watershed-management-pei (accessed on Nov 22, 2019).

9. López-Urrea, R.; Martín de Santa Olalla, F.; Fabeiro, C.; Moratalla, A. Testing evapotranspiration equations using lysimeter observations in a semiarid climate. *Agric. Water Manag.* **2006**, *85*, 15–26.
10. Abdullah, S.S.; Malek, M.A.; Abdullah, N.S.; Kisi, O.; Yap, K.S. Extreme Learning Machines: A new approach for prediction of reference evapotranspiration. *J. Hydrol.* **2015**, *527*, 184–195.
11. Allen, R.G.; Pereira, L.S.; Raes, D.; Smith, M. Crop evapotranspiration-Guidelines for computing crop water requirements-FAO Irrigation and drainage paper 56. **1998**.
12. Yin, Y.; Wu, S.; Zheng, D.; Yang, Q. Radiation calibration of FAO56 Penman-Monteith model to estimate reference crop evapotranspiration in China. *Agric. Water Manag.* **2008**, *95*, 77–84.
13. Shih, S.F. Data Requirement for Evapotranspiration Estimation. *J. Irrig. Drain. Eng.* **1984**, *110*, 263–274.
14. Cigizoglu, H.K. Estimation, forecasting and extrapolation of river flows by artificial neural networks. *Hydrol. Sci. J.* **2009**, *48*, 361.
15. Firat, M. Comparison of Artificial Intelligence Techniques for river flow forecasting. *Hydrol. Earth Syst. Sci.* **2008**, *12*, 123–139.
16. Wang, Y.-M.; Traore, S.; Kerh, T. Monitoring Event-Based Suspended Sediment Concentration by Artificial Neural Network Models. *WSEAS Trans. Comput.* **2008**, *7*.
17. Kumar, M.; Raghuwanshi, N.S.; Singh, R.; Wallender, W.W.; Pruitt, W.O. Estimating Evapotranspiration using Artificial Neural Network. *J. Irrig. Drain. Eng.*

2002, *128*, 224–233.

18. Sudheer, K.P.; Gosain, A.K.; Ramasastri, K.S. Estimating Actual Evapotranspiration from Limited Climatic Data Using Neural Computing Technique. *J. Irrig. Drain. Eng.* **2003**, *129*, 214–218.
19. Aytek, A.; Guven, A.; Yuce, M.I.; Aksoy, H. An explicit neural network formulation for evapotranspiration. *Hydrol. Sci. J.* **2008**, *53*, 893–904.
20. Rahimikhoob, A. Estimation of evapotranspiration based on only air temperature data using artificial neural networks for a subtropical climate in Iran. *Theor. Appl. Climatol.* **2010**, *101*, 83–91.
21. Patil, A.P.; Deka, P.C. An extreme learning machine approach for modeling evapotranspiration using extrinsic inputs. *Comput. Electron. Agric.* **2016**, *121*, 385–392.
22. Feng, Y.; Jia, Y.; Cui, N.; Zhao, L.; Li, C.; Gong, D. Calibration of Hargreaves model for reference evapotranspiration estimation in Sichuan basin of southwest China. *Agric. Water Manag.* **2017**, *181*, 1–9.
23. Kisi, O.; Cengiz, T.M. Fuzzy Genetic Approach for Estimating Reference Evapotranspiration of Turkey: Mediterranean Region. *Water Resour. Manag.* **2013**, *27*, 3541–3553.
24. Lipton, Z.C.; Berkowitz, J.; Elkan, C. A Critical Review of Recurrent Neural Networks for Sequence Learning. **2015**.
25. Tawegoum R; Belbrahem R; Chasseriaux G Modeling Evapotranspiration Prediction on Nursery Area Using Rrecurrent Neural Networks. In Proceedings of the Fifth International Workshop on Artificial Intelligence in Agriculture, Cairo,

Egypt.

26. Hochreiter, S.; Schmidhuber, J. Long Short-Term Memory. *Neural Comput.* **1997**, *9*, 1735–1780.
27. Schuster, M.; Paliwal, K.K. Bidirectional recurrent neural networks. *IEEE Trans. Signal Process.* **1997**, *45*, 2673–2681.
28. Kratzert, F.; Klotz, D.; Brenner, C.; Schulz, K.; Herrnegger, M. Rainfall-runoff modelling using Long Short-Term Memory (LSTM) networks. *Hydrol. Earth Syst. Sci.* **2018**, *22*, 6005–6022.
29. Hu, C.; Wu, Q.; Li, H.; Jian, S.; Li, N.; Lou, Z. Deep learning with a long short-term memory networks approach for rainfall-runoff simulation. *Water* **2018**, *10*, 1–16.
30. Zhang, J.; Zhu, Y.; Zhang, X.; Ye, M.; Yang, J. Developing a Long Short-Term Memory (LSTM) based model for predicting water table depth in agricultural areas. *J. Hydrol.* **2018**, *561*, 918–929.
31. Ladlani, I.; Houichi, L.; Djemili, L.; Heddam, S.; Belouz, K. Modeling daily reference evapotranspiration (ET0) in the north of Algeria using generalized regression neural networks (GRNN) and radial basis function neural networks (RBFNN): A comparative study. *Meteorol. Atmos. Phys.* **2012**, *118*, 163–178.
32. Feng, Y.; Cui, N.; Zhao, L.; Hu, X.; Gong, D. Comparison of ELM, GANN, WNN and empirical models for estimating reference evapotranspiration in humid region of Southwest China. *J. Hydrol.* **2016**, *536*, 376–383.
33. Natural Resources Canada. Water balance - derived precipitation and evapotranspiration. Available online: https://open.canada.ca/data/en/dataset/910100c0-4f8c-5ae8-ae87-69bf230e43cf

(accessed on Feb 1, 2020).

34. Planting Calendar: When to Plant Vegetables. Available online: https://www.almanac.com/gardening/planting-calendar/PE/charlottetown (accessed on Feb 2, 2020).

35. Feng, Y.; Peng, Y.; Cui, N.; Gong, D.; Zhang, K. Modeling reference evapotranspiration using extreme learning machine and generalized regression neural network only with temperature data. *Comput. Electron. Agric.* **2017**, *136*, 71–78.

36. Afzaal, H.; Farooque, A.A.; Abbas, F.; Acharya, B.; Esau, T. Groundwater Estimation from Major Physical Hydrology Components Using Artificial Neural Networks and Deep Learning. *Water* **2019**, *12*, 5.

37. Reddy, S.V..; Reddy, K.T.; ValliKumari, V. Optimization of Deep Learning Using Various Optimizers, Loss Functions And Dropout. *Int. J. Recent Technol. Eng.* **2018**, *7*.

38. Mohan, A.T.; Gaitonde, D. V. A Deep Learning based Approach to Reduced Order Modeling for Turbulent Flow Control using LSTM Neural Networks. *arXiv Prepr. arXiv* **2018**, *1804.09269*.

39. Food and Agriculture Organization of the United Nations Available online: http://www.fao.org/news/archive/news-by-date/2011/en/ (accessed on Nov 17, 2019).

40. Fabeiro, C.; Martín De Santa Olalla, F.; De Juan, J.A. Yield and size of deficit irrigated potatoes. *Agric. Water Manag.* **2001**, *48*, 255–266.

41. Gurdian, T. Potatoes: A billion dollar industry for P.E.I. *2012*.

42. Statistics Canada Potato Market Information Review 2013-2014 - Agriculture and Agri-Food Canada (AAFC). **2015**.

43. Bélanger, G.; Walsh, J.R.; Richards, J.E.; Milburn, P.H.; Ziadi, N. Yield response of two potato cultivars to supplemental irrigation and N fertilization in New Brunswick. *Am. J. Potato Res.* **2000**, *77*, 11–21.

44. Porter, G.A.; Opena, G.B.; Bradbury, W.B.; McBurnie, J.C.; Sisson, J.A. Soil management and supplemental irrigation effects on potato: I. Soil properties, tuber yield, and quality. *Agron. J.* **1999**, *91*, 416–425.

45. Kashyap, P.S.; Panda, R.K. Evaluation of evapotranspiration estimation methods and development of crop-coefficients for potato crop in a sub-humid region. *Agric. Water Manag.* **2001**, *50*, 9–25.

46. Onder, S.; Caliskan, M.E.; Onder, D.; Caliskan, S. Different irrigation methods and water stress effects on potato yield and yield components. *Agric. Water Manag.* **2005**, *73*, 73–86.

47. Stylianou, Y.; Orphanos, P.I. Irrigation of potatoes by sprinklers or tricklers on the basis of pan evaporation in a semi-arid region. *Potato Res.* **1981**, *24*, 159–170.

48. Ünlü, M.; Kanber, R.; Şenyigit, U.; Onaran, H.; Diker, K. Trickle and sprinkler irrigation of potato (Solanum tuberosum L.) in the Middle Anatolian Region in Turkey. *Agric. Water Manag.* **2006**, *79*, 43–71.

49. WFD-CIS *Guidance document on the application of water balances for supporting the implementation of WFD*; 2015;

50. Ierna, A.; Mauromicale, G. Potato growth, yield and water productivity response to different irrigation and fertilization regimes. *Agric. Water Manag.* **2018**, *201*, 21–

26.

51. FAO Potato: Food and Agriculture Organization of the United Nations Available online: http://www.fao.org/land-water/databases-and-software/crop-information/potato/en/ (accessed on Jan 28, 2020).

52. Pereira, L.S.; Cordery, I.; Iacovides, I. Improved indicators of water use performance and productivity for sustainable water conservation and saving. *Agric. Water Manag.* **2012**, *108*, 39–51.

53. Food and Agriculture Organizations of United Nations Potato. Available online: http://www.fao.org/land-water/databases-and-software/crop-information/potato/en/ (accessed on Nov 17, 2019).

54. Jiang, Y.; Somers, G.; Mutch, J. Application of Numerical Modeling To Groundwater Assessment and Management in Prince Edward Island. In Proceedings of the 57th Canadian Geotechnical Conference; 2004; Vol. 57, pp. 2–9.

55. Gao, Z.; Long, D.; Tang, G.; Zeng, C.; Huang, J.; Hong, Y. Assessing the potential of satellite-based precipitation estimates for flood frequency analysis in ungauged or poorly gauged tributaries of China's Yangtze River basin. *J. Hydrol.* **2017**, *550*, 478–496.

56. USGS Available online: https://www.sciencedaily.com/releases/2012/11/121116124557.htm (accessed on Dec 12, 2019).

57. Francis, R.M. *Hydrogeology of the winter river basin-Price Edward Island*; 1989;

58. Mohammadi, K. Groundwater Table Estimation Using MODFLOW and Artificial Neural Networks. In *Practical Hydroinformatics*; Springer Berlin Heidelberg:

Berlin, Heidelberg, 2008; pp. 127–138.

59. Rajaee, T.; Ebrahimi, H.; Nourani, V. A review of the artificial intelligence methods in groundwater level modeling. *J. Hydrol.* **2019**, *572*, 336–351.

60. Mohanty, S.; Jha, M.K.; Kumar, A.; Panda, D.K. Comparative evaluation of numerical model and artificial neural network for simulating groundwater flow in Kathajodi–Surua Inter-basin of Odisha, India. *J. Hydrol.* **2013**, *495*, 38–51.

61. Karandish, F.; Šimůnek, J. A comparison of numerical and machine-learning modeling of soil water content with limited input data. *J. Hydrol.* **2016**, *543*, 892–909.

62. Zhang, N.; Shen, S.L.; Zhou, A.; Xu, Y.S. Investigation on Performance of Neural Networks Using Quadratic Relative Error Cost Function. *IEEE Access* **2019**, *7*, 106642–106652.

63. Sarir, P.; Shen, S.L.; Wang, Z.F.; Chen, J.; Horpibulsuk, S.; Pham, B.T. Optimum model for bearing capacity of concrete-steel columns with AI technology via incorporating the algorithms of IWO and ABC. *Eng. Comput.* **2019**.

64. Atangana Njock, P.G.; Shen, S.L.; Zhou, A.; Lyu, H.M. Evaluation of soil liquefaction using AI technology incorporating a coupled ENN / t-SNE model. *Soil Dyn. Earthq. Eng.* **2020**, *130*.

65. Elbaz, K.; Shen, S.-L.; Zhou, A.; Yuan, D.-J.; Xu, Y.-S. Optimization of EPB Shield Performance with Adaptive Neuro-Fuzzy Inference System and Genetic Algorithm. *Appl. Sci.* **2019**, *9*, 780.

66. Sahoo, S.; Jha, M.K. Groundwater-level prediction using multiple linear regression and artificial neural network techniques: a comparative assessment Sasmita.

Hydrogeol. J. **2013**, *21*, 1865–1887.

67. Kouziokas, G.N.; Chatzigeorgiou, A.; Perakis, K. Multilayer Feed Forward Models in Groundwater Level Forecasting Using Meteorological Data in Public Management. *Water Resour. Manag.* **2018**, *32*, 5041–5052.
68. Juan, C.; Genxu, W.; Tianxu, M. Simulation and prediction of suprapermafrost groundwater level variation in response to climate change using a neural network model. *J. Hydrol.* **2015**, *529*, 1211–1220.
69. Coulibaly, P.; Anctil, F.; Aravena, R.; Bobée, B. Artificial neural network modeling of water table depth fluctuations. *Water Resour. Res.* **2001**, *37*, 885–896.
70. Mueller, J.; Park, J.; Sahu, R.; Varadharajan, C.; Arora, B.; Faybishenko, B.; Agarwal, D. Surrogate Optimization of Deep Neural Networks for Groundwater Predictions. **2019**.
71. Maheshwara Babu, B.; Srinivasa Reddy, G.; Satishkumar, U.; Kulkarni, P. Simulation of Groundwater Level Using Recurrent Neural Network (RNN) in Raichur District, Karnataka, India. *Int.J.Curr.Microbiol.App.Sci* **2018**, *7*, 3358–3367.
72. Lähivaara, T.; Malehmir, A.; Pasanen, A.; Kärkkäinen, L.; Huttunen, J.M.J.; Hesthaven, J.S. Estimation of groundwater storage from seismic data using deep learning. *Geophys. Prospect.* **2019**, *67*, 2115–2126.
73. Ravansalar, M.; Rajaee, T. Evaluation of wavelet performance via an ANN-based electrical conductivity prediction model. *Environ. Monit. Assess.* **2015**, *187*.
74. Krishna, B.; Satyaji Rao, Y.R.; Vijaya, T. Modelling groundwater levels in an urban coastal aquifer using artificial neural networks. *Hydrol. Process.* **2008**, *22*, 1180–

1188.

75. Tsanis, I.K.; Coulibaly, P.; Daliakopoulos, I.N. Improving groundwater level forecasting with a feedforward neural network and linearly regressed projected precipitation. *J. Hydroinformatics* **2008**, *10*, 317–330.

76. Gholami, V.; Chau, K.W.; Fadaee, F.; Torkaman, J.; Ghaffari, A. Modeling of groundwater level fluctuations using dendrochronology in alluvial aquifers. *J. Hydrol.* **2015**, *529*, 1060–1069.

77. Safeeq, M.; Fares, A. Groundwater and Surface Water Interactions in Relation to Natural and Anthropogenic Environmental Changes. In *Emerging Issues in Groundwater Resources*; Springer International Publishing, 2016; pp. 289–326.

78. Lee, S.; Lee, K.K.; Yoon, H. Using artificial neural network models for groundwater level forecasting and assessment of the relative impacts of influencing factors. *Hydrogeol. J.* **2019**, *27*, 567–579.